Zoological Journal of the Linnean Society, 2022, **196**, 1608–1636. With 7 figures.

The common bottlenose dolphin (*Tursiops truncatus*) ecotypes of the western North Atlantic revisited: an integrative taxonomic investigation supports the presence of distinct species

ANA P. B. COSTA[1*†], WAYNE MCFEE[2], LYNSEY A. WILCOX[3], FREDERICK I. ARCHER[4] and PATRICIA E. ROSEL[3]

[1]*Department of Biology, University of Louisiana at Lafayette, 410 East St. Mary Boulevard, Lafayette, LA 70503, USA*
[2]*National Centers for Coastal Ocean Science, National Oceanic and Atmospheric Administration (NOAA) National Ocean Service, 331 Fort Johnson Road, Charleston, SC 29412, USA*
[3]*National Marine Fisheries Service, Southeast Fisheries Science Center, 646 Cajundome Boulevard, Lafayette, LA 70506, USA*
[4]*National Marine Fisheries Service, Southwest Fisheries Science Center, 8901 La Jolla Shores Drive, La Jolla, CA 92037, USA*

Received 1 November 2021; revised 16 February 2022; accepted for publication 21 February 2022

Integrative taxonomy can help us to gain a better understanding of the degree of evolutionary divergence between taxa. In the western North Atlantic (wNA), two ecotypes (coastal and offshore) of common bottlenose dolphin, *Tursiops truncatus*, exhibit some external morphological differences, and previous genetic findings suggested that they could be different species. However, their taxonomy remains unsettled. Using an integrative approach comparing traditional and geometric morphometrics, mitochondrial and nuclear DNA, we evaluated evolutionary relationships between these ecotypes. We observed congruence among these lines of evidence, strongly indicating that the wNA ecotypes are following distinct evolutionary trajectories. Based on mitochondrial DNA analyses, we detected significant divergence (Nei's $d_A = 0.027$), unshared haplotypes and one fixed difference leading to complete diagnosability (percentage diagnosable = 100%) of the wNA coastal ecotype. We found morphological diagnosability and negligible nuclear gene flow between the wNA ecotypes. Integration of these multiple lines of evidence revealed that the wNA coastal ecotype is an independent evolutionary unit, appearing to be more closely related to coastal dolphins in the Gulf of Mexico and Caribbean Sea than to their parapatric offshore neighbours, while the offshore dolphins form a relatively cohesive worldwide unit, *T. truncatus*. We propose that this coastal ecotype is recognized as a distinct species, resurrecting the name *Tursiops erebennus*.

ADDITIONAL KEYWORDS: cetaceans – genetics – morphometrics – speciation – taxonomy.

INTRODUCTION

Accurate taxonomy is essential for a better understanding of biodiversity and ecological interactions and to design effective conservation efforts. However, 'taxonomic inflation', the raising of populations or subspecies to species through application of different species concepts (Issac *et al.*, 2004), can cause considerable taxonomic instability. It can have negative implications for conservation, because it can give a false impression of high biodiversity in localized areas by the erroneous description of more species. It can also increase the number of threatened species by increasing endemism while reducing population sizes (Agapow *et al.*, 2004; Issac *et al.*, 2004). Thus,

*Corresponding author. E-mail: anapbccosta@gmail.com
†Current address: Rosenstiel School of Marine and Atmospheric Science (RSMAS), University of Miami, 1365 Memorial Drive, Coral Gables, FL 33146, USA
[Version of record, published online 13 May 2022; http://zoobank.org/ urn:lsid:zoobank.org:pub:C4BBB151-A36C-4B55-AC20-9AB5F52B9424]

accurate taxonomy is crucial for effective evaluation and conservation of biodiversity.

Many different species concepts have been proposed, but none is accepted universally (see Wilkins, 2009; Hausdorf, 2011). The concept applied in a particular study can be taxon specific or even data specific. De Queiroz (2007) argued that there is a clear distinction between how species are differentiated (species delimitation) and how species are defined (species concept). Although species concepts differ in the criteria used to delimit species, all agree that a species is: 'a separately evolving lineage composed of a population or collection of populations' (de Queiroz, 2007, as modified by Taylor *et al.*, 2017b). Recognizing this, the unified species concept decouples the species definition from the delimitation criterion (de Queiroz, 2007). In this concept, the different criteria used by the different species concepts (e.g. reproductive isolation, phenotypic differentiation and phylogenetic difference) should be considered lines of evidence (secondary properties) used to assess species divergence, but not necessary properties for conceptualization of a species. However, when examining these different lines of evidence, the question is raised: how do we know when populations have diverged 'enough' in a given line of evidence to be considered a separately evolving, independent lineage, hence a separate species?

Integrative taxonomy attempts to address this question by using an interdisciplinary approach to provide more rigorous criteria when delimiting species (e.g. Dayrat, 2005; Padial *et al.*, 2010; Schlick-Steiner *et al.*, 2010). Although a single line of evidence can be used to suggest species divergence, multiple independent lines of evidence are favoured because individual lines can each have their shortcomings. A single line of evidence can have high classification error rates and under- or overestimate species numbers (Dayrat, 2005; de Queiroz, 2007; Padial *et al.*, 2010; Schlick-Steiner *et al.*, 2010; Taylor *et al.*, 2017a). For example, morphology-based evidence can overestimate the number of species owing to intraspecific variation (e.g. phenotypic plasticity and sexual dimorphism), whereas genetic evidence can underestimate because of incomplete lineage sorting or hybridization (see Schlick-Steiner *et al.*, 2010). Taking these potential problems into consideration, several guidelines (e.g. Padial *et al.*, 2010; Schlick-Steiner *et al.*, 2010; Taylor *et al.*, 2017a) and statistical methods (e.g. Knowles & Carstens, 2007; Archer *et al.*, 2017b; Rosel *et al.*, 2017) have been developed to improve the species delineation process.

Taylor *et al.* (2017a) provided guidelines and quantitative methods to help secure taxonomic stability and accuracy when delimiting cetacean taxa based on mitochondrial DNA (mtDNA) control region sequence data. Their delimitation criteria combined a measure of divergence coupled with the degree of diagnosability based on a heritable character (Taylor *et al.*, 2017b). For the measure of divergence, Nei's d_A was found to be useful in identifying thresholds of divergence for cetacean subspecies and species (see Rosel *et al.*, 2017) and a percentage diagnosable threshold was also identified (see Archer *et al.*, 2017b). However, as highlighted by the authors, for species delimitation, additional lines of evidence, such as nuclear DNA and/or non-genetic data (e.g. morphology) should be used to support the evolutionary divergence seen in mtDNA to discard the possibility of male-mediated gene flow not detectable using mtDNA data alone (Taylor *et al.*, 2017a).

Multiple independent lines of evidence, including haematological profiles (Duffield *et al.*, 1983), parasite load (Mead & Potter, 1990), skull morphology (Mead & Potter, 1995; Toledo, 2013), genetics (Hoelzel *et al.*, 1998; Kingston & Rosel, 2004; Rosel *et al.*, 2009; Louis *et al.*, 2021) and distribution (Torres *et al.*, 2003; Waring *et al.*, 2009), suggest that two ecotypes (coastal and offshore) of common bottlenose dolphins, *Tursiops truncatus* (Montagu, 1821), in the western North Atlantic (wNA) might be different species. However, these previous studies investigating differences between the wNA ecotypes usually considered only a single line of evidence and have not examined congruence among different types of data, such as morphology and genetics, using the same specimens.

Here, we take an integrative taxonomic approach to revisit the evolutionary distinctiveness of the two common bottlenose dolphin ecotypes in the wNA and help to clarify their taxonomic status. Using different morphological and genetic analyses, applied (where possible) to the same specimens, we evaluate whether these ecotypes should be delimited as distinct populations, subspecies or species and examine their evolutionary relationships to bottlenose dolphins found elsewhere in the world.

MATERIAL AND METHODS

MORPHOLOGICAL AND TRADITIONAL MORPHOMETRIC ANALYSES

Samples

A total of 147 physically mature skulls and 43 vertebral columns of *T. truncatus* were examined. Some of these skulls were also examined in previous morphological studies (Mead & Potter, 1995; J. Mead, personal communication: 36 skulls in common; Toledo, 2013: 66 skulls in common). The specimens were collected between 1966 and 2011 along the east coast of the USA during stranding, capture/relocation and

incidental catch events (Fig. 1). Most of the stranded animals had no live locality information, although two samples were photo-identified as resident dolphins of South Carolina estuarine waters, seven originated from bycatch or capture/relocation in waters < 1 km of the coast, and seven were collected in offshore waters (i.e. estimated as > 100 km from shore based on geographical coordinates; Supporting Information, Table S1).

We examined only skulls defined as physically mature (i.e. cranially mature), approximated by fusion (i.e. no movement) of the maxillae to the cranium (Ross & Cockcroft, 1990) and rostral fusion, which here was considered based on ≥ 90% fusion of the premaxilla to the maxilla over the length of the rostrum (Jordan *et al.*, 2015). Of the 43 specimens for which both the skull and the complete or nearly complete postcranial skeletons were available, 28 also exhibited a physically mature vertebral column (pattern 3, following Costa & Simões-Lopes, 2012). All 43 postcranial skeletons were used to define the vertebral formula, but only 21 of the 28 physically mature vertebral columns were measured (seven exhibited broken or fused vertebral structures).

Type specimens of the two *Tursiops* Gervais, 1855 species previously described from the east coast of the USA were also examined. The first was the physically mature, but incomplete, vertebral column (missing the last caudal vertebrae) of the holotype *Tursiops erebennus* (Cope, 1865), deposited in the Academy of Natural Sciences of Drexel University (museum number: *ANSP 3020*). There are no records of a skull of *T. erebennus*. The second was the skull and vertebral column of the female syntype of *Tursiops subridens* True, 1884, deposited in the Smithsonian National Museum of Natural History. There are two *T. subridens* specimens, a female (*USNM A 16505*) and a male *(USNM A 16504)*. Neither syntype was considered physically mature (their skulls did not fit the requirements presented above), and only the female

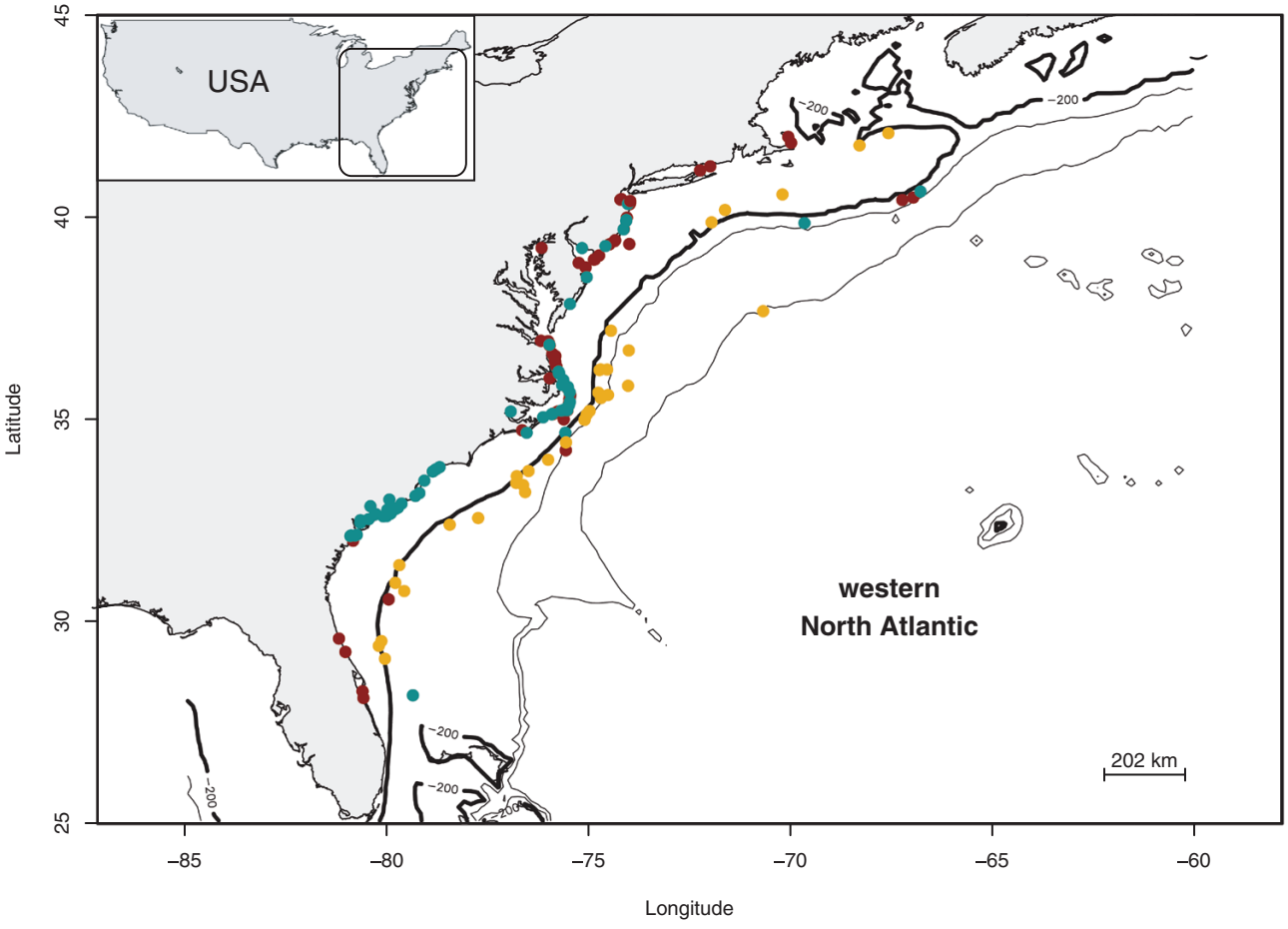

Figure 1. Map of the western North Atlantic study area showing the sampling locations of samples with only morphological data available (brown), with morphological and genetic data available (cyan) or with only genetic data available (gold). The 200 m isobath line is shown in bold black. Thin black lines represent the 2000 and 4000 m isobaths.

skull was measured, because the male was considered younger (see True, 1889: 36) and was not used in the multivariate analyses. Nevertheless, both female and male syntypes were considered when estimating the vertebral formula of *T. subridens*. We also examined the skull of the holotype *T. truncatus* deposited in the Natural History Museum, London, UK (*NHMUK 353a*), which was collected in English waters. There are no records of a vertebral column from this holotype. All morphological statistical analyses described below were conducted in R v.4.1.0 (R Core Team, 2021).

Comparative anatomy of the skull: a priori stratification

The two ecotypes in the wNA appear to partition the habitat, with the coastal ecotype present primarily in estuarine and nearshore coastal and shelf waters and the offshore ecotype present primarily at the continental shelf break (depths usually > 100 m; Torres *et al.*, 2003; Hayes *et al.*, 2017). Drawing from some of the cranial features previously identified by Mead & Potter (1995) and Toledo (2013), we examined skulls known to have come from coastal (N = 9) or offshore (N = 7) waters to identify morphological characters that could help to differentiate the ecotypes visually. Based on this examination, we identified five characteristics of skull morphology (described below) that consistently distinguished the two ecotypes and used them to conduct an a priori assignment of the remaining wNA skulls (N = 131) to the offshore or coastal ecotype (Table 1).

Offshore characters: As observed from the left lateral view (Supporting Information, Fig. S1A): (1) cranial vertex flat (anterior end of the nasals at the same height or slightly shorter than the other components of the cranial vertex); (2) elongated lacrimal, with its anterior end slender and extending beyond the anterior end of the ascending process of maxilla; and (3) marked convex pharyngeal crest. As observed from the ventral view (Supporting Information, Fig. S1B): (4) intermediate to wider vomer when compared with the posterior process of the pterygoids; and (5) posterior border of the pterygoid hamuli oriented almost 90° to the sagittal plane of the skull.

Coastal characters: As observed from left lateral view (Supporting Information, Fig. S1C): (1) cranial vertex elevated (anterior end of the nasals at slightly higher height than the other components of the cranial vertex); (2) shorter lacrimal, with its anterior end more flat (square shaped) and ending before the anterior end of the ascending process of maxilla (usually, the latter is fully covering the anterior end of the lacrimal, which ends almost at the same height as the preorbital process of the frontal); and (3) straight (non-convex) pharyngeal crest. As observed from the ventral view (Supporting Information, Fig. S1D): (4) intermediate to narrower vomer when compared with the posterior process of the pterygoids; and (5) posterior border of the pterygoid hamuli in an acute angle to the sagittal plane of the skull.

Multivariate analyses

Cranial and vertebral column measurements were taken with dial and digital callipers by A.P.B.C. to the nearest millimetre, following the descriptions by Costa *et al.* (2016) (Supporting Information, Table S2). Assembly of the vertebral column and vertebral counts were performed to define the vertebral formula for the wNA samples, including the holotype *T. erebennus* and syntypes of *T. subridens* (following Costa *et al.*, 2016).

We first performed a random forest (RF) analysis using the R package *rfPermute* v.2.5 (Archer, 2021) to examine clustering of the samples based on cranial multivariate analyses. This RF clustering was performed to assign the 131 skulls of unknown live locality to ecotype and quantify the accuracy of the a priori stratifications. To conduct this analysis, we first created a classification model with the 16 samples of known live locality. For this model, we used a total of 25 cranial variables: the five qualitative variables used in the a priori

Table 1. Number of bottlenose dolphin samples from the western North Atlantic used in the different analyses (i.e. lines of evidence)

	M	TM	GM	VC	VCm	nDNA	mtDNA	TS
N (P)	147 (100)	147 (100)	90 (61.2)	43 (29.3)	21 (14.3)	78*,† (53.1)	78* (53.1)	147 (100)

*This total does not include the 37 biopsy samples collected in offshore waters of the western North Atlantic. The total number of samples used in the genetic analyses when including the biopsied specimens is N = 115 (see main text).
†A total of 11 of the 78 samples failed to amplify up to 18 loci and were not used in the downstream analyses.
Abbreviations: GM, geometric morphometrics (skull); M, a priori morphological stratification (skull); mtDNA, mitochondrial DNA control region; *N*, number of samples; nDNA, nuclear microsatellites; P, percentage of the total number of samples (TS) used in the respective line of evidence; TM, traditional morphometrics (skull); TS, total number of bottlenose dolphin samples from the western North Atlantic used in this study; VC, morphological classification of the vertebral column based on vertebral formula; VCm, morphological classification of the vertebral column based on morphometrics.

stratifications, with the respective classification values as offshore or coastal for each variable (see above); the presence or absence of scars of parasitic nematodes in the genus *Crassicauda* sp. Leiper & Atkinson, 1914 (variable abbreviation CRCA); and (listed in Supporting Information, Table S2). We then used this model to predict the ecotype assignment probabilities of each of the 131 skulls. The number of variables chosen at each split (*mtry*) was set to eight and the number of trees (*ntree*) to 20 000, which produced stable classification models in initial runs. Balanced models were generated by setting *sampsize* to half of the smallest sample size, and samples were selected for each tree without replacement.

In addition, using all 25 cranial variables, we performed an unsupervised clustering of skulls to identify the number of natural clusters and compare this clustering with the a priori and RF classifications. We used the density clustering (DC) algorithm (Rodrigues & Laio, 2014) as implemented in the R package *densityClust* v.0.3 (Pedersen *et al.*, 2017). This method initially identifies peaks of clusters by computing the local density (ρ) of each individual and its distance (δ) to the nearest individual of higher density based on a matrix of pairwise Euclidean distances calculated using the 25 cranial variables, which are scaled using the R function *scale* before performing this analysis because it is a distance-based analysis. Individuals are then assigned to a cluster based on the nearest peak of higher density (Rodrigues & Laio, 2014). We performed a clustering with all 147 skulls, where the *densityClust* parameters were set to $\rho = 1.427$ and $\delta = 5.216$ after evaluation of the decision graph, which showed an inflection in the density distribution with the number of clusters defined based on the position of the smallest peak in the graph (Supporting Information, Fig. S2A).

We then evaluated the ordination of the scaled cranial variables ($N = 25$) with a principal components analysis (PCA) implemented in the R function *prcomp*. The distribution of the identified clusters (defined from the a priori, RF and DC results), highlighted with 95% confidence ellipses, was visualized along the first two principal components (PCs).

Lastly, for the cranial analyses, we conducted a second RF analysis with all the samples ($N = 147$) and the 25 cranial variables (not scaled owing to the nature of RF, which is a tree-based model and does not require scaling to normalize the data) to assess their relative importance to classification accuracy using the mean decrease in accuracy metric (Liaw & Wiener, 2002). The samples were assigned to a cluster before the analysis according to the congruence of the results of the previous analyses. The most significant important variables were identified with 1000 permutation replicates to create a null distribution of importance scores, from which *P*-values were estimated. Other RF parameters were defined as described above.

We conducted similar unsupervised clustering (density clustering) analyses using the vertebral data of physically mature specimens ($N = 21$) without missing data for the selected vertebral measurements. Of the original 35 vertebral measurements taken in this study, eight were omitted owing to excessive missing values across individuals examined (Supporting Information, Table S2), leaving a total of 27 measurements for the following analyses. The DC settings followed the descriptions above, with a few modifications: $\rho = 1.392$ and $\delta = 4.344$ (Supporting Information, Fig. S2B). We then conducted a supervised RF analysis based on the DC classifications of the 21 samples, using the 27 vertebral measurements, to evaluate the assignment scores of the samples. We also assessed the relative importance of the vertebral data to classification accuracy using the mean decrease in accuracy metric (Liaw & Wiener, 2002). The RF parameters were defined as described above.

Sexual dimorphism

We investigated sexual dimorphism in the cranial data to evaluate whether it might influence the clustering classifications. This test was conducted by creating RF models to quantify the degree to which sex could be classified as a function of the 25 cranial variables. We initially created one model using all skulls with sex information ($N = 140$; ♀ = 79, ♂ = 61), followed by one model for each ecotype as defined by the clustering classifications above (coastal: ♀ = 58, ♂ = 41; offshore: ♀ = 21, ♂ = 20). Balanced models were created by randomly selecting the same number of samples for each sex without replacement for each tree in the RF using *balancedSampsize*. For each model, *ntree* was set to 20 000 and *mtry* was set to either eight (all and coastal models) or four (offshore model). We also assessed the relative importance (with estimated *P*-values) of the measurements for each model using the mean decrease in accuracy metric and with a total of 1000 permutation replicates run for each RF model. We also evaluated whether the presence of sexual dimorphism within each ecotype (see Results) is influencing the detected differentiation between the ecotypes (i.e. whether the ecotype differentiation is dependent on the sex in question). This was achieved by visually representing, in violin plots, the differences between the ecotypes and sexes based on 19 cranial measurements. Violin plots were built using the R package *ggplot2* v.3.3.4 (Wickham, 2016), and mean and standard deviation values were estimated in the violin plots for each ecotype per sex.

Univariate analyses

For each skull (where possible), we also recorded the tooth/alveolus counts for each tooth row in the maxilla (TUL: $N = 147$; TUR: $N = 145$) and mandible (TLL and TLR: $N = 143$). We then estimated the median difference between the ecotypes based on the tooth counts for each tooth row and performed a non-parametric Kolmogorov–Smirnov test (KS test) to examine its significance.

We also constructed a receiver operating characteristic (ROC) curve to evaluate the diagnostic ability of classifying the ecotypes based on tooth counts (per tooth row). An ROC curve was constructed for each tooth row by plotting the true-positive rate (TPR) against the false-positive rate (FPR). The TPR represents the proportion of observations that were correctly predicted as positive among all positive observations, whereas the FPR is the proportion of observations that were incorrectly predicted as positive among all positive observations. We calculated an ROC curve for each unique cut-off value of number of teeth. The TPR was then estimated as the fraction of coastal samples that have tooth counts higher than or equal to the cut-off, whereas the FPR was estimated as the fraction of offshore samples that have tooth counts higher than or equal to the cut-off.

We also recorded the tooth width (WTH), measured (where possible) from a tooth at the midlength of the left maxilla in each skull sample ($N = 89$). To test for differences between the ecotypes, we conducted two non-parametric tests using the R functions *wilcox.test* or *kruskal.test*. The Wilcoxon–Mann–Whitney test (conducted by lumping the sexes within each ecotype; $N = 89$) and the Kruskal–Wallis test (conducted by separating the sexes within each ecotype; $N = 87$; two samples were excluded because the sex was unknown) were used because the variable WTH failed to meet the normality and homogeneity assumptions for conducting a two-way ANOVA.

Information about the total external body length (TL) was available from field measurements for 142 of the 147 dolphins, including the 28 specimens with physically mature vertebral columns. The TL was also available for *T. erebennus* (considered physically mature) and *T. subridens*, but they were not included in the following statistical tests. Differences in TL between ecotypes were first tested using samples ($N = 28$) considered physically mature on the vertebral column (i.e. a mark of fully physically mature specimens), to avoid confounding effects of maturity in the statistical analysis. We performed a two-way ANOVA using the R function *aov*, taking into consideration the ecotype, sex and their interaction. The ANOVA sum of squares (SS) was calculated for types II and III using the function *Anova* in the R package *car* v.3.0.11 (Fox & Weisberg, 2019). We then performed a KS test for all the samples with TL information ($N = 142$), independently from the maturity of the vertebral column, to evaluate whether the wNA ecotypes have identical distributions in body length, using the function *ks.test* in the R package *dgof* v.1.2 (Arnold & Emerson, 2011). We also represented visually in violin plots the differences between the ecotypes associated with body length for all the samples with TL and sex information ($N = 139$; three samples with TL were excluded because the sex was unknown). Mean and standard deviation values were estimated in the violin plots for each ecotype per sex. Further significant differences in distribution in body length between sexes within each ecotype were tested with a KS test.

Holotypes

We used RF models to classify the three type specimens (*T. truncatus*, *T. subridens* and *T. erebennus*) to wNA ecotype. A model was created to classify each type specimen using only the variables available for the specimen under consideration and the samples with no missing values for these variables [*T. truncatus*: 24 cranial variables (the cranial measurement WZP was missing because of a broken structure); *T. subridens*: 25 cranial variables; *T. erebennus*: ten vertebral measurements (only the vertebral column was available for this holotype, but it was partly mounted, which allowed the measurement of only the two lumbar vertebrae, L1 and L8)]. For the trained model for the assignment of *T. subridens*, we used only females of known live locality ($N = 12$) because the sex of this syntype was known (i.e. female) and we detected sexual dimorphism in each ecotype based on traditional morphometrics (see results). The trained model for the assignment of *T. truncatus* was conducted by combining the sexes of all samples of known live locality ($N = 16$) because the sex information was not available for this holotype. For *T. erebennus*, owing to the small number of samples ($N = 3$) of known live locality with information available for the ten vertebral measurements used, the trained model was built using all samples ($N = 19$) with these measurements and lumping the sexes because there was no sex information available for this holotype. The RF parameters were the same as described above for the cranial multivariate analyses using the R package *rfPermute*.

Geometric morphometric analyses

Samples

To evaluate differences between the wNA ecotypes associated with the size and shape of the skull, we performed a three-dimensional geometric morphometric

(GM) analysis using 23 cranial landmarks (Supporting Information, Table S3) and 90 of the 147 skulls (Table 1; Supporting Information, Table S1). Of these 90 samples, 84 had sex information available (♀ = 44; ♂ = 40). All landmarks were assumed to be homologous in all specimens and were collected using a three-dimensional digitizer (MicroScribe G2X, Immersion Corporation) available at the Smithsonian Institution's Museum Support Center. The landmarks were assessed on the left side of each skull to avoid possible confounding effects of the asymmetry in odontocete skulls.

Statistical analyses

Procrustes superimposition was used to transform the measured point coordinates into Procrustes (shape) coordinates by removing position, size and rotation of the landmarks (Rohlf & Slice, 1990) in the R package *geomorph* v.4.0.0 (Adams *et al.*, 2021) using the function *gpagen*. This method removes the effect of differences in size between the measured objects by centring all object shapes at an origin, scaling all shapes to the same unit size and rotating each shape around the origin until the sum of square distance between them is minimized (Rohlf, 1999). The Procrustes (shape) coordinates were used as variables of the skull shape in the downstream analyses, whereas centroid size (the square root of the sum of the square distances of all the landmarks from their centre of gravity) was used as a proxy for skull size. Further downstream analyses were also conducted using the R package *geomorph*, unless otherwise stated.

We evaluated the influence of sexual dimorphism on skull shape (Procrustes coordinates) and size [natural logarithm of the centroid size (lnCS)] by performing a two-way Procrustes ANOVA with the function *procD.lm* (1000 permutations) and examining the sex and ecotype interaction. A total of six individuals (three from each ecotype group) were removed before this analysis because their sexes were unknown. Further pairwise comparisons were conducted using the function *pairwise* of the R package *RRPP* v.1.0.0 (Collyer & Adams, 2018), using the distance between least-squares (LS) means, to evaluate how ecotypes differ in shape and/or size, accounting for the sex effect.

We tested whether allometric patterns (i.e. the relationship between size and shape) differed between the ecotypes using a two-way Procrustes ANOVA, with the models of common and unique allometries constructed using the function *procD.lm* (1000 permutations). Given that we found a heterogeneous pattern (i.e. the allometric slopes differed significantly between ecotypes; see Results), we did not follow the residual approach (which uses size-free shape residuals) and retained the allometric variation in the downstream analyses. We then evaluated the magnitude and direction of allometric shape changes between the ecotypes using the function *pairwise*. We tested for differences in trajectory magnitude (the amount of shape change per unit of lnCS) based on vector lengths and tested for differences in the direction of allometric shape change based on angular differences in slopes. We also performed a three-way Procrustes ANOVA with *procD.lm* (1000 permutations) to summarize the previous analyses by testing simultaneously the effects of skull size, ecotypes, sex and their interactions.

A PCA was then conducted using the function *gm.prcomp* to investigate the differences associated with skull shape between coastal and offshore ecotypes in the wNA following the ecotype classification obtained with the traditional morphometric analyses (above). The clusters were highlighted with 95% confidence ellipses. After the PCA, we performed a two-way ANOVA on each of the first two PC axes to test for the effects of ecotype, sex and their interaction on shape variation using the R function *aov*. We also evaluated the classification of the ecotypes according to shape differences using RF (*rfPermute*) and all 62 PCs, with the parameters as described above.

Genetic analyses

Samples

Tissues were available for 78 of the specimens used in the morphological analyses (Table 1; Fig. 1; Supporting Information, Table S1). Additionally, bone powder was obtained from the vertebral body of the lumbar vertebra of the holotype *T. erebennus* (*ANSP 3020*). Past attempts to amplify and sequence bone DNA of both syntypes of *T. subridens* (*USNM A 16504* and *USNM A 16505*) have failed. Therefore, this type could not be included in the present genetic analyses. We also examined 37 biopsy samples collected in offshore waters of the wNA (Fig. 1; Supporting Information, Table S1), with the objective of examining whether there is correlation between the morphological data and the biopsy samples (i.e. whether molecular profiles of biopsy samples collected in offshore waters would cluster with those of stranding samples exhibiting an offshore morphology). The soft tissues were stored in 20% salt-saturated dimethyl sulfoxide (Amos & Hoelzel, 1991) or 90–100% ethanol. For a detailed description of the DNA extraction and molecular sexing of the samples, see the Supporting Information, section 'DNA extraction and sexing'.

Microsatellite genotyping and analyses

Nuclear genetic diversity was examined for all soft tissue samples (N = 115) collected in the wNA using 19

microsatellite loci amplified in four multiplexes using a Qiagen Type-it Microsatellite PCR kit, with the PCR conditions described in the Supporting Information (Table S4). Genotyping was performed on an ABI 3130 Genetic Analyzer with GeneScan 500 LIZ size standard and viewed with GeneMapper v.5 (Applied Biosystems). Quality control was applied to all microsatellite genotyping to ensure consistency across PCR amplification and genotyping runs by including no-DNA and positive controls in all PCRs. Individuals were kept in the analyses when ≥ 18 loci were successfully amplified (N = 104), resulting in a decrease of 10% of the initial sample size. The genotyping error rate was estimated by randomly selecting 10% of the individuals and re-genotyping at all 19 loci.

The presence of duplicate samples in the data set was investigated using MSTools (Park, 2001). Genotyping errors attributable to null alleles, allelic dropout and incorrect scoring of stutter peaks were checked using MICRO-CHECKER v.2.2.3 (Van Oosterhout *et al.*, 2004), with 10 000 iterations. Each locus was also tested for departure from Hardy–Weinberg equilibrium (HWE) (Guo & Thompson, 1992) and linkage disequilibrium using the Fisher's exact tests with the program GENEPOP v.4.6 (Rousset, 2008), using 10 000 dememorizations, 1000 batches and 10 000 iterations per batch. Both tests were applied considering the full final data set and to the ecotype groups separately [individuals were assigned to an ecotype based on their clustering according to the skull morphology (above) or sample origin for the biopsy samples]. The sequential Bonferroni technique (Holm, 1979) was applied to correct for multiple tests.

Evidence for more than one genetic cluster (K) in the wNA was investigated using the Bayesian clustering programs TESS v.2.3.1 (Durand *et al.*, 2009) and STRUCTURE v.2.3.4 (Pritchard *et al.*, 2010) for 104 samples, following the parameter settings described by Costa *et al.* (2021). Congruence of the results from these two approaches was evaluated as a means to interpret the reliability in the determination of the clusters.

Inbreeding coefficients (F_{IS}) and mean observed (H_O) and expected (H_E) heterozygosities within, in addition to pairwise F_{ST} (Weir & Cockerham, 1984) between the genetically identified clusters (with 10 000 permutations), were estimated using ARLEQUIN v.3.5.1.2 (Excoffier & Lischer, 2010). Mean allelic richness (AR) was estimated using FSTAT v.2.9.3 (Goudet, 1995); the total number of alleles (NA) and total number of private alleles per cluster were identified using CONVERT (Glaubitz, 2004).

BayesAss v.3.0.4 (Wilson & Rannala, 2003) was used to estimate levels and directionality of contemporary gene flow between the genetically identified clusters, following Costa *et al.* (2021). The default step length was modified to 0.30 for two mixing parameters (Δa, allele frequencies; Δf, inbreeding coefficients) to obtain acceptance rates between 20 and 60% (acceptance rates obtained:Δm, migration rates = 0.24, Δa = 0.29 and Δf = 0.23), as suggested by Rannala (2015). We also compared the posterior densities with the prior densities (using the option -p) to check the level of informativeness in the data (Rannala, 2015).

Lastly, mean pairwise relatedness values (r) were estimated for each of the genetic clusters using the R package *related* (Pew *et al.*, 2015) with R v.3.6.2 (R Core Team, 2019). Using observed allele frequencies, simulations of 500 pairs for four relationship types (parent–offspring, full-sibling, half-sibling and unrelated) were conducted using four moment estimators (Queller & Goodnight, 1989; Li *et al.*, 1993; Lynch & Ritland, 1999; Wang, 2002) and two likelihood-based estimators (Milligan, 2003; Wang, 2007) to determine the most appropriate relatedness estimator for each cluster. The relatedness estimator with the highest Pearson correlation coefficient was then used to estimate r between members within each genetic cluster. To exclude the possibility that kinship might be overestimating the population structure, we repeated the clustering analyses, current gene flow estimations and nuclear F_{ST} estimation excluding one sample from each pair of individuals with high relatedness values ($r \geq 0.45$) within each genetic cluster.

Mitochondrial DNA sequencing and analyses

A 354 bp portion of the mtDNA control region was amplified and sequenced for all 115 soft tissue samples. Samples were amplified using the primers L15824 (Rosel *et al.*, 1999) and H16498 (Rosel *et al.*, 1994), following Costa *et al.* (2021) for soft tissue samples. The DNA extracted from the holotype *T. erebennus* was successfully amplified and sequenced using smaller overlapping fragments and nested PCRs to produce the full 354 bp fragment (Supporting Information, section 'mtDNA sequencing - bone DNA'). The haplotype of the holotype *T. erebennus* was used only in the analyses of genetic relationship based on mtDNA data. Negative and positive controls were used in all PCRs for quality control. All PCR products were purified using low-melting point agarose gel extraction and agarase digestion. All samples were sequenced in both directions using Applied Biosystems BigDye Terminator v.1.1 cycle sequencing kit and an ABI 3130 Genetic Analyzer. Forward and reverse reads of all samples were edited using GENEIOUS v.11.0 (https://www.geneious.com), with a consensus sequence of the two reads being created for each sample. BLASTN (http://blast.ncbi.nlm.nih.gov/Blast.cgi) was used to examine the best matches of species identity to the mtDNA sequences obtained in this study.

Statistical analyses of the mtDNA sequences were conducted after removal of samples identified as duplicates based on the nuclear analyses. ARLEQUIN was used to estimate the mtDNA haplotype (Nei & Tajima, 1981) and nucleotide (Nei, 1987) diversities, and genetic differentiation between the wNA ecotypes as identified by the genetic clustering analyses (described above) using the metrics F_{ST} and Φ_{ST} (conducted with and without closely related individuals). Net between-group nucleotide divergence (d_A; Nei, 1987) was estimated using the R package *strataG* v.2.0.2 (Archer *et al.*, 2017a). The best model of evolution to estimate divergence was identified using jModelTest v.2.1.6 (Posada, 2008) and the Bayesian information criterion (BIC) on the CIPRES Science Gateway (Miller *et al.*, 2010): Hasegawa–Kishino–Yano (Hasegawa *et al.*, 1985) with invariant sites. We did not include in these statistical analyses (with the exception of the percentage diagnosable analysis, see below) four samples with heteroplasmic (hpl) haplotypes (following Vollmer *et al.*, 2011) owing to the software limitations in dealing with ambiguous bases.

We also estimated the percentage diagnosable (PD) based on an RF procedure (Archer *et al.*, 2017b) to create classification models to check for subspecies- or species-level diagnosability between the wNA ecotypes using all 115 mtDNA sequences obtained in this study. We followed the 95% diagnosability threshold for subspecies and 100% for species recommended for cetaceans by Taylor *et al.* (2017a). The sequences were reduced to only variable sites ($N = 28$), with the exclusion of the unique substitutions as recommend by Archer *et al.* (2017b) because they are considered uninformative. An RF balanced model was conducted using the *rfPermute* package, with previously described settings.

In addition, the new control region sequences were aligned using CLUSTALW implemented in Geneious and default parameters with 74 mtDNA control region haplotypes previously found in common bottlenose dolphin ecotypes of the wNA and available in GenBank (see Supporting Information, Table S5). We conducted this procedure as a way of identifying wNA haplotypes in our data set that were previously identified genetically as coastal or offshore ecotypes. A median joining network of the wNA mtDNA haplotypes obtained in this study was constructed using the program NETWORK v.5.0.0.3 (Bandelt *et al.*, 1999), with default parameters, to examine relationships among the haplotypes found in the wNA and the holotype *T. erebennus*.

Worldwide comparison

Morphological analyses: The skulls from the wNA ($N = 147$) were compared morphologically with skulls of *T. truncatus* collected elsewhere ($N = 169$; including the holotype) with a PCA (conducted as described above) using the (ln-transformed, natural log transformation) cranial measurements ($N = 18$) available for all samples ($N = 316$). The additional samples came from seven different main oceanographic regions, and they were highlighted in the PCA plot following their oceanographic region and type classification (Supporting Information, Table S6), according to the present study and previous ones, when available (cf. Perrin *et al.*, 2011; Costa *et al.*, 2021; A. P. B. Costa, F. I. Archer, P. E. Rosel, & W. F. Perrin, unpublished data). The clusters identified based on the type classifications were highlighted with 95% confidence ellipses and visualized along the first two PCs.

We also conducted an unsupervised DC analysis based on this worldwide data set (i.e. 316 skulls and 18 cranial measurements). The DC analysis was performed with the 18 (ln-transformed) variables and *densityClust* parameters set as $\rho = 13.33$ and $\delta = 0.449$ after observation of the position of the cluster peaks in the decision graph (Supporting Information, Fig. S2C).

Mitochondrial DNA phylogeny: We constructed a maximum likelihood tree to investigate phylogenetic relationships among a subset of the wNA data set ($N = 27$ haplotypes) and 222 *Tursiops* sp. haplotypes acquired from GenBank (Supporting Information, Table S7) representing several other oceanographic regions [e.g. Caribbean Sea, Gulf of Mexico (GOMx), Indian Ocean, Pacific Ocean, Gulf of California, western South Atlantic (wSA), eastern North Atlantic (eNA), Mediterranean Sea and Black Sea]. We highlight that we included in this data set the mtDNA control region haplotypes obtained for 12 of the 18 samples from the northern GOMx used in the worldwide morphological analyses described above. These GOMx mtDNA haplotypes are listed in the Supporting Information (Table S7) as from the 'Gulf of Mexico (U.S.A.)' and they were obtained from the same area (GOMx) in previous studies (Sellas *et al.*, 2005; Vollmer & Rosel, 2017; P. E. Rosel, personal communication; see Supporting Information, Table S7). *Lagenorhynchus acutus* (Gray, 1828) (GenBank accession number EF092934) and *Steno bredanensis* (G. Cuvier in Lesson, 1828) (GenBank accession number DQ845437) were used as outgroups. Given that some GenBank sequences were shorter than 354 bp (present study), the final control region alignment created using CLUSTALW was 311 bp. The maximum likelihood tree was constructed using the IQ-TREE web server (Trifinopoulos *et al.*, 2016) with ultrafast bootstrap (UFBoot; Minh *et al.*, 2013) analysis, with 1000 bootstrap replicates, 200 iterations for the IQ-TREE stopping rule and all other default parameters. The Shimodaira–Hasegawa-like

approximate likelihood ratio test (SH-aLRT; Guindon *et al.*, 2010) with 1000 bootstrap replicates was also performed to compare branch support values between SH-aLRT and UFBoot. As recommended in IQ-TREE documentation, a clade is typically considered true for UFBoot values ≥ 95% (Minh *et al.*, 2013) and SH-aLRT values ≥ 80% (Guindon *et al.*, 2010). The best evolutionary model for DNA substitution was selected using JMODELTEST and BIC–TMP3uf ('3-parameter model with unequal frequencies'; Posada, 2008) with invariant sites and gamma. Tree visualization was performed using FIGTREE v.1.4.3 (http://tree.bio.ed.ac.uk/software/figtree/) with a bootstrap (UFBoot) cut-off value of 80%, because UFBoot achieves more unbiased support values (Minh *et al.*, 2013).

RESULTS

MORPHOLOGICAL ANALYSES

The a priori stratification of the wNA skulls to ecotype, using the five qualitative morphological characters, separated the data set into 45 offshore and 102 coastal dolphins. A subset of the skulls in our data set has been used in previous morphological studies (Mead & Potter, 1995; J. Mead, personal communication: $N = 36$; Toledo, 2013: $N = 66$), and our a priori stratification was 100% congruent with the classifications used in these studies (Supporting Information, Table S1). It is important to highlight that our a priori analysis was not based on the full set of characters used in the previous studies. Although we found some degree of variation, especially in the orientation of the pterygoid hamuli (Supporting Information, Table S8), the a priori stratification provided by the five qualitative morphological characters (when used together) was highly consistent with the multivariate classifications based on RF and DC analyses (see below).

Random forest analysis (based on 25 unscaled cranial variables) assigned all 16 samples of known live locality to the same ecotype as defined by the location from where they were collected (bycatch or capture/relocation) or photo-identified as residents (coastal, $N = 9$; offshore, $N = 7$; Supporting Information, Table S9). The RF analysis also separated the 131 samples of unknown live locality into 93 coastal and 38 offshore, with 100% congruence with the ecotype classification based on the a priori stratification.

The decision graph of the unsupervised clustering based on the cranial DC analysis pointed to the presence of three peaks of higher density (Supporting Information, Fig. S2A), which suggested the existence of three clusters based on the 25 scaled cranial variables (Supporting Information, Fig. S3): one cluster composed of all samples classified by RF as coastal ($N = 102$), a second cluster with the majority of the samples classified by RF as offshore ($N = 38$) and a third cluster ('cluster-3') with seven samples classified by RF as offshore. It is noteworthy that these seven samples formed a potential third cluster owing to their similarity based on the cranial variables analysed (see below), but they were also placed together with the other 38 offshore samples in the DC plot of point distribution (i.e. multidimensional scaling plot) based also on their similarity to the other offshore samples (Supporting Information, Fig. S3).

Two clusters were identified in the PCA plot according to the first two PCs (72.88% of the variance): one cluster representing the coastal samples and the second representing the offshore samples, including the seven-sample cluster from the DC analysis (Supporting Information, Fig. 2A). Most of the differentiation between the ecotypes is on PC1, with all 25 variables being positively correlated, whereas the separation of the ecotypes along PC2 seems to be linked with variables associated with skull shape and presence/absence of *Crassicauda* sp. scars (Supporting Information, Table S10).

Scars from *Crassicauda* sp. were observed in 46.67% ($N = 21$) of the samples classified as offshore by RF analyses ($N = 45$) and in only 1.96% ($N = 2$) of the samples classified as coastal ($N = 102$). All seven offshore samples of 'cluster-3' from the DC analysis presented such scars. Their puzzling classification based on the DC analysis seems to be caused by a combination of the size of their skull [they are among the smallest RF offshore skulls; condylobasal length (CBL) ranging from 469 to 489 mm] and the orientation of their pterygoid hamuli (posterior border at a more acute angle compared with the majority of the RF offshore samples). Despite their unusual combination of characteristics, the results provided by the classification analyses together (including the position of the samples in the DC-multidimensional scaling plot; Supporting Information, Fig. S3) do not validate the presence of a third cluster among our data set. Therefore, taken together, our findings indicate 100% congruence in the clustering classifications of all the different analyses, separating the data set into 102 coastal samples and 45 offshore samples.

The cranial variables of most significant importance highlighted by RF as the best at explaining the differentiation between the ecotypes were the first four qualitative characters (i.e. except the orientation of the pterygoid hamuli) and measurements of overall length (CBL) and width (PW, PROW, POW and WZP) of the skull, length (LR, LRIN) of the rostrum, width of the internal nares (WIN) and length of the antorbital process of the left lacrimal (LAOLL) (Supporting Information, Table S11). The offshore ecotype presented higher values in all the cranial measurements than

the coastal ecotype (i.e. offshore dolphins have overall larger skulls; Supporting Information, Table S12).

Most of the offshore specimens ($N = 19$) had the vertebral formula $C_7 + T_{13} + L_{15–16} + Ca_{27–29} = 62–65$, with one exception for the thoracic region (T_{14}) and another two for the lumbar section (L_{17}). The coastal samples ($N = 21$) showed lower counts in each region (except the cervical), with the vertebral formula $C_7 + T_{12} + L_{14–15} + Ca_{26–28} = 59–61$. The unsupervised DC analyses (based on 27 vertebral measurements) classified all 21 physically mature individuals with 100% congruence with the cranial classifications (Supporting Information, Fig. S4). The supervised RF analysis confirmed the accuracy in the DC classifications, with high classification votes (≥ 70%; Supporting Information, Table S9). The most important vertebral measurements separating the ecotypes were associated mainly with the overall length of the vertebrae (measured from the tips of transverse processes) and width of the neural arch (Supporting Information, Table S13), with higher values for the offshore dolphins.

When evaluating sexual dimorphism of the cranial variables, we observed strong evidence for differences in skull morphology based on sex, considering the whole data set and within each ecotype (Supporting Information, Table S14). The most significant cranial measurements differentiating males and females in the full data set and within each ecotype were overall width of the skull (WZP, PROW and POW) and rostrum (WRH) (Supporting Information, Table S15). Nevertheless, when examining the differences in each cranial measurement [here, we considered only the morphometric variables ($N = 19$) and not the qualitative variables of the skull] according to ecotype and sex, we noticed that males were larger than females within each ecotype and, overall, offshore samples were larger than the coastal samples, regardless of the sex (Supporting Information, Table S16). This was true for most of the variables, including all those considered of significant importance in separating the ecotypes (Supporting Information, Fig. S5). Therefore, although there is sexual dimorphism within each ecotype, this finding does not influence the strong differentiation detected between the wNA ecotypes.

Overall, the maxilla presented slightly more teeth than the mandible in both ecotypes. Significant differences ($P < 0.003$) in the median number of teeth between the ecotypes were detected only in the mandible (TLL and TLR), with coastal samples tending to have one more tooth ($N = 23$) than offshore samples ($N = 22$) (Supporting Information, Table S17). According to the graphical output of the ROC curve analysis, no optimum diagnostic cut-off value was detected to differentiate the ecotypes based on the number of teeth in the maxilla (Supporting Information, Fig. S6). The best cut-off value for both tooth rows in the mandible was 23, but it was not considered a good classifier. A good classifier would have a high TPR (closer to one) and a low FPR (closer to zero), but here we obtained a relatively low TPR (TLL = 0.8; TLR = 0.76) and relatively high FPR (TLL and TLR = 0.43) (Supporting Information, Fig. S6). Overall, coastal (mean, 6.3 mm) and offshore (mean, 6.1 mm) dolphins presented similar tooth width, and no significant differences were detected between the ecotypes when either lumping the sexes (Wilcoxon test = 687; $P = 0.6773$) or comparing each ecotype based on sex (KW $\chi^2 = 0.20273$; d.f. = 3; $P = 0.9771$).

The physically mature offshore dolphins (based on vertebral column) were significantly larger in external total body length (mean, 287.07 cm) compared with the coastal specimens (mean, 256.15 cm) regardless of the sex ($P < 0.01$; Supporting Information, Table S18). No significant differentiation was detected when considering the sex or the ecotype–sex interaction ($P > 0.05$; Supporting Information, Table S18), indicating that there is no sexual dimorphism in total body length when examining only the specimens considered as physically mature based on the vertebral column ($N = 28$). When considering all samples ($N = 142$) with TL information (i.e. using both physically mature and immature samples according to the vertebral columns and those without vertebral column information), we also detected significant differences in the distributions in body length between the ecotypes (KS test = 0.615; $P = 10^{-10}$). However, in contrast to the above analysis using only physical mature samples as defined by the vertebral columns ($N = 28$), when considering the full data set ($N = 142$), we observed some indication of sexual dimorphism according to the violin plots, with males possibly being larger than females in total body length in both offshore (mean ♂, 298.25 cm; mean ♀, 273.71 cm) and coastal groups (mean ♂, 261.66 cm; mean ♀, 247.53 cm). This pattern was reinforced when examining the distributions in body length between sexes within each ecotype using the full data set ($N = 142$), where we detected significant values within each ecotype (coastal: KS test = 0.447; $P = 0.00015$; offshore: KS test = 0.605; $P = 0.001$) (Fig. 2B).

Using the holotypes, the random forest analyses assigned *T. erebennus* (based on ten vertebral measurements and 19 samples) and *T. subridens* (based on 25 cranial variables and 12 females of known live locality) to the coastal ecotype with 97.3 and 91.99% probability, respectively (Supporting Information, Table S19). The *T. truncatus* holotype (based on 24 cranial variables and 16 samples of known live locality) was assigned to the offshore ecotype with 92.1% probability (Supporting Information, Table S19). Total external body lengths for the holotypes *T. erebennus*

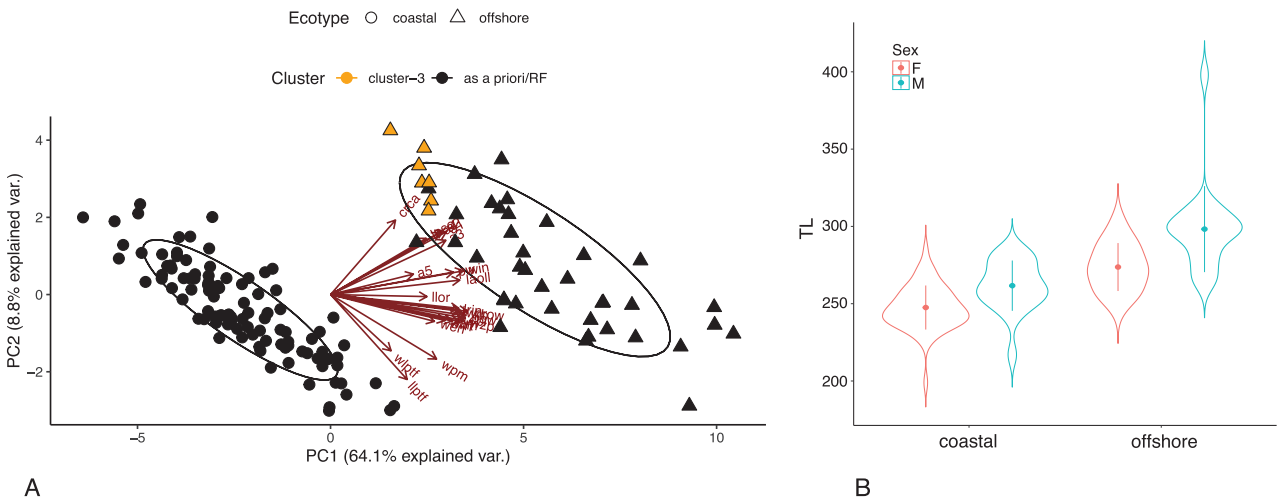

Figure 2. Traditional morphometric analyses of bottlenose dolphins of the western North Atlantic. A, scatter plot of the principal component 1 (PC1) and 2 (PC2) scores from the analysis of 25 cranial variables and 147 samples. Ellipses correspond to the 95% confidence interval. The shape of the data points represents the ecotype (coastal or offshore) as defined based on random forest (RF) results. The colour of the data points represents the clustering classifications according to density clustering (DC) results: black, samples follow the same classification (coastal or offshore) as RF and the a priori stratification; orange, 'cluster-3' identified only by DC (see main text). B, violin plot of the total external body length (TL) differentiated per sex (F, female; M, male) and ecotype.

and *T. subridens* (female) were reported as 228.6 and 230 cm, respectively. Both are slightly smaller than the mean size observed for the coastal ecotype (physically mature individuals, $N = 13$: 256.15 cm; all samples with TL, $N = 99$: 253.55 cm). The holotype *T. erebennus* ($C_7 + T_{12} + L_{14} + Ca_{14+}$) and the syntypes *T. subridens* (*USNM A 16504* and *USNM A 16505*: $C_7 + T_{12} + L_{14} + Ca_{26} = 59$) also have a vertebral formula similar to the coastal ecotype. Neither body length information nor a vertebral formula was available for the holotype *T. truncatus*.

Geometric morphometric analyses

The geometric morphometric analysis for sexual dimorphism showed a significant effect of ecotype alone, sex alone and ecotype–sex interaction on skull shape (Table 2). However, when considering sexual dimorphism of skull size, we observed a significant effect only for ecotype (Table 2). Further pairwise comparisons indicated that offshore dolphins differed significantly from coastal dolphins in skull shape, independent of the sex under comparison. No significant differences were observed between sexes within each ecotype (Table 3).

We observed a significant interaction term between lnCS and ecotype (Supporting Information, Table S20), which led us to reject the null hypothesis of common allometry (equal slopes), and we assumed that the ecotypes differ in allometric trajectory (Fig. 3A). We found a significant pairwise absolute difference (d) between slope vector lengths ($d = 0.12$; $P = 0.04$), suggesting that the ecotypes differ in allometric trajectory magnitude (the amount of change in shape with growth). A significant difference was also observed in angular slopes (76.6°; $P = 0.006$), indicating that ecotypes also differ in the direction in which shape changes with growth. Additionally, the three-way Procrustes ANOVA displayed congruence in the detected differences in shape variables and allometric trajectories between ecotypes, but not between sexes (Supporting Information, Table S21).

The first two PCs of the PCA for the geometric morphometric analysis of skull shape explained 39.19% of the variation (Fig. 3B). A clear separation between the two wNA ecotypes was observed along the first principal component (PC1; 29.96% of total variance), which was confirmed by the ANOVA results: a significant effect of ecotype (SS = 0.062; $F = 445.88$; d.f. = 1; $P < 10^{-16}$) and ecotype–sex interaction (SS = 0.001; $F = 5.08$; d.f. = 2; $P = 0.008$). The second principal component (PC2; 9.23%) indicated a possible separation based on sex, but with shape overlap occurring between the sexes within each ecotype (Fig. 3B); this result is also congruent with the ANOVA results: a significant effect of sex (SS = 0.005; $F = 14.52$; d.f. = 2; $P < 10^{-6}$) and ecotype–sex interaction (SS = 0.002; $F = 5.74$; d.f. = 2; $P = 0.005$). The most marked changes in shape associated with PC1 and PC2 (Fig. 3B) demonstrated that with an increase in PC1 score (from coastal to

Table 2. Two-way Procrustes ANOVA testing the influence of sexual dimorphism on skull shape (Procrustes coordinates) and skull size (lnCS) of bottlenose dolphins of the western North Atlantic according to ecotype (coastal and offshore), sex (females and males) and their interaction

		d.f.	SS	MS	R^2	F	Z	P-value
Skull shape	Ecotype	1	0.023566	0.0235656	0.10309	11.8811	6.0678	**0.001**
	Sex	1	0.004229	0.0042295	0.01850	2.1324	2.8912	**0.003**
	Ecotype–sex interaction	1	0.005037	0.0050371	0.02204	2.5396	3.1440	**0.002**
	Residuals	80	0.158676	0.0019834	0.69415	–	–	–
	Total	83	0.228591	–	–	–	–	–
Skull size	Ecotype	1	0.08703	0.087030	0.258686	69.1040	5.1734	**0.001**
	Sex	1	0.00407	0.004069	0.012094	3.2308	1.4396	0.066
	Ecotype–sex interaction	1	0.00174	0.001739	0.005169	1.3808	0.7280	0.258
	Residuals	80	0.10075	0.001259	0.299475	–	–	–
	Total	83	0.33643	–	–	–	–	–

Significant P-values are in bold. Number of permutations: 1000. Sum of squares (SS) and cross-products: type III. MS: mean squares.

Table 3. *Post hoc* pairwise comparisons of sexual dimorphism on skull shape (Procrustes coordinates) of bottlenose dolphins of the western North Atlantic according to ecotype (coastal and offshore), sex (females and males) and their interaction

	Female, coastal	Male, coastal	Female, offshore	Male, offshore
Female, coastal	–	0.978	**0.001**	**0.001**
Male, coastal	0.01781043	–	**0.001**	**0.001**
Female, offshore	0.04968680	0.05582569	–	0.079
Male, offshore	0.06080124	0.06364596	0.03207639	–

Pairwise shape differences (Procrustes distances) are below the diagonal, with their respective P-values (from 1000 random permutations) above the diagonal. Significant P-values are in bold.

offshore), there was a dorsoventral expansion of the braincase, and the occipital region had a more dorsal position and orientation. The lacrimal was elongated, as was the cranial vertex, with the anterior end of the nasals at a lower height than the other components of the cranial vertex. An increase in PC2 score (from males to females) resulted in a slightly dorsoventral compression of the braincase and narrowing of the occipital region. The rostrum was more elongated.

The RF results based on geometric morphometrics (GM) exhibited 97.8% congruence with the ecotype assignments based on the traditional morphometric analyses (Supporting Information, Table S22). Only two samples (one from each ecotype) were classified by GM-RF to the opposite ecotype based on skull shape (both with low classification votes, < 65%). Both samples (USNM504096 and USNM572261) are females of unknown live locality collected as strandings in New Jersey. Previous cranial multivariate analyses classified these samples as offshore (USNM504096) and coastal (USNM572261). However, as seen in the GM-PCA plot (Fig. 3B; Supporting Information, Fig. S7), these two samples are at the edge of the 95% confidence ellipses of their respective predefined ecotype (assigned based on traditional morphometrics) and are also found close to the ellipsis of the opposite ecotype (assigned by the GM-RF results). Given that the GM-RF analysis was performed based on the principal components, the RF classification of these two samples could be a reflection of their positions along the PCA plot, where the higher variance between the clusters is explained by the first principal component.

Genetic analyses

Genotyping of 18 or 19 loci was successful for 104 of the 115 samples; no duplicate samples were found, and no errors were identified when re-genotyping 10% of the samples. Significant departure from HWE (after Bonferroni correction, $P < 0.003$), linkage disequilibrium (after Bonferroni correction, $P < 0.0003$) and the presence of null alleles were detected for several microsatellite loci when considering all the samples as a single population. However, no significant values were observed when dividing the data set into the two defined ecotypes based on morphological analyses and sampling

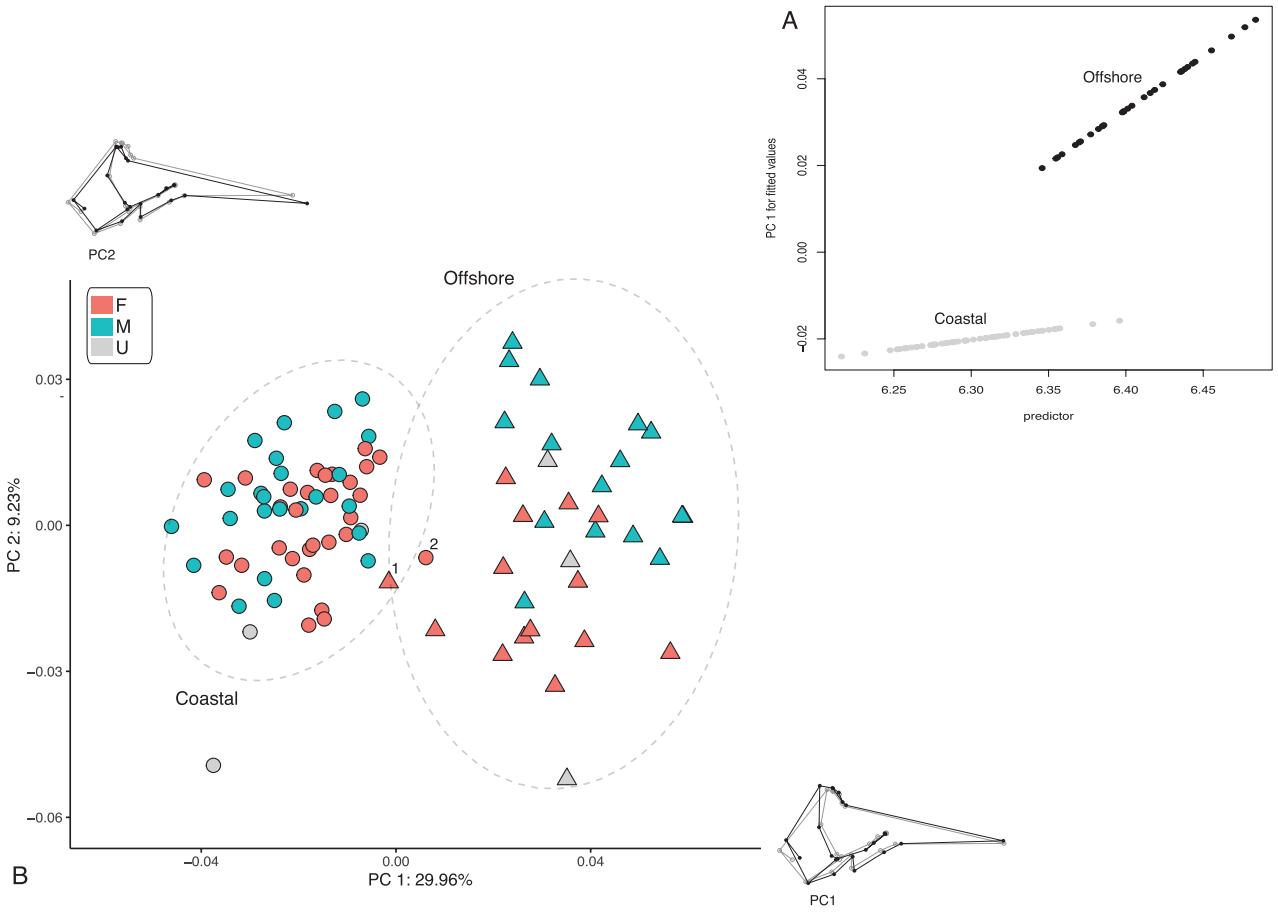

Figure 3. Three-dimensional geometric morphometric (GM) analyses of bottlenose dolphins of the western North Atlantic. A, allometry plot of predicted lines based on fitted values (unique allometries model) to visualize how shape allometry varies by ecotype. The PredLine method calculates fitted values from the *procD.lm* fit and plots the first principal component of the predicted values against size, i.e. lnCS (see Adams & Nistri, 2010). B, scatter plot of the principal component 1 (PC1) and 2 (PC2) scores based on 23 cranial landmarks and 90 samples. Ellipses correspond to the 95% confidence interval. Samples are differentiated by sex (F, female; M, male; U, unknown) and ecotype. The mean specific shape variation along PC1 (bottom right) and PC2 (top left) is also shown. Grey represents the mean shape, whereas black represents the change in shape from the mean shape. Sample 1, USNM504096; sample 2, USNM572261.

location, suggesting a Wahlund effect (Garnier-Géré & Chikhi, 2013) when pooling samples from the two ecotypes. The dyadic likelihood estimator (dyadml; Milligan, 2003) was the best relatedness estimator for both genetic clusters and was used to determine *r*. High relatedness values were observed only within the coastal cluster with four related pairs (one sample was in common for two pairs). No relevant changes were observed in the clustering analyses after the removal of three individuals from the related coastal samples (data not shown). Therefore, we kept all samples in the subsequent analyses. The mtDNA control region was amplified and sequenced successfully for all 115 wNA soft tissue samples and for the holotype *T. erebennus*. The final genetic data set (soft tissue samples) was composed of 52 males and 63 females.

The clustering analyses (TESS and STRUCTURE) based on the nuclear microsatellite data supported subdivision of the wNA samples into two clusters (Fig. 4A, B). In both TESS and STRUCTURE, the most likely number of clusters was identified as $K = 2$ (Supporting Information, Fig. S8), with high assignment probabilities for all individuals (TESS > 98%; STRUCTURE > 90%). The genetic clustering was consistent with the morphological classifications: one genetic cluster was composed of samples previously assigned to the coastal ecotype by the skull morphology, and the second cluster was composed of samples classified as offshore by morphology and the specimens biopsied in offshore waters (i.e. > 100 km from shore). We also examined the plots based on $K = 3$, and a third potential cluster

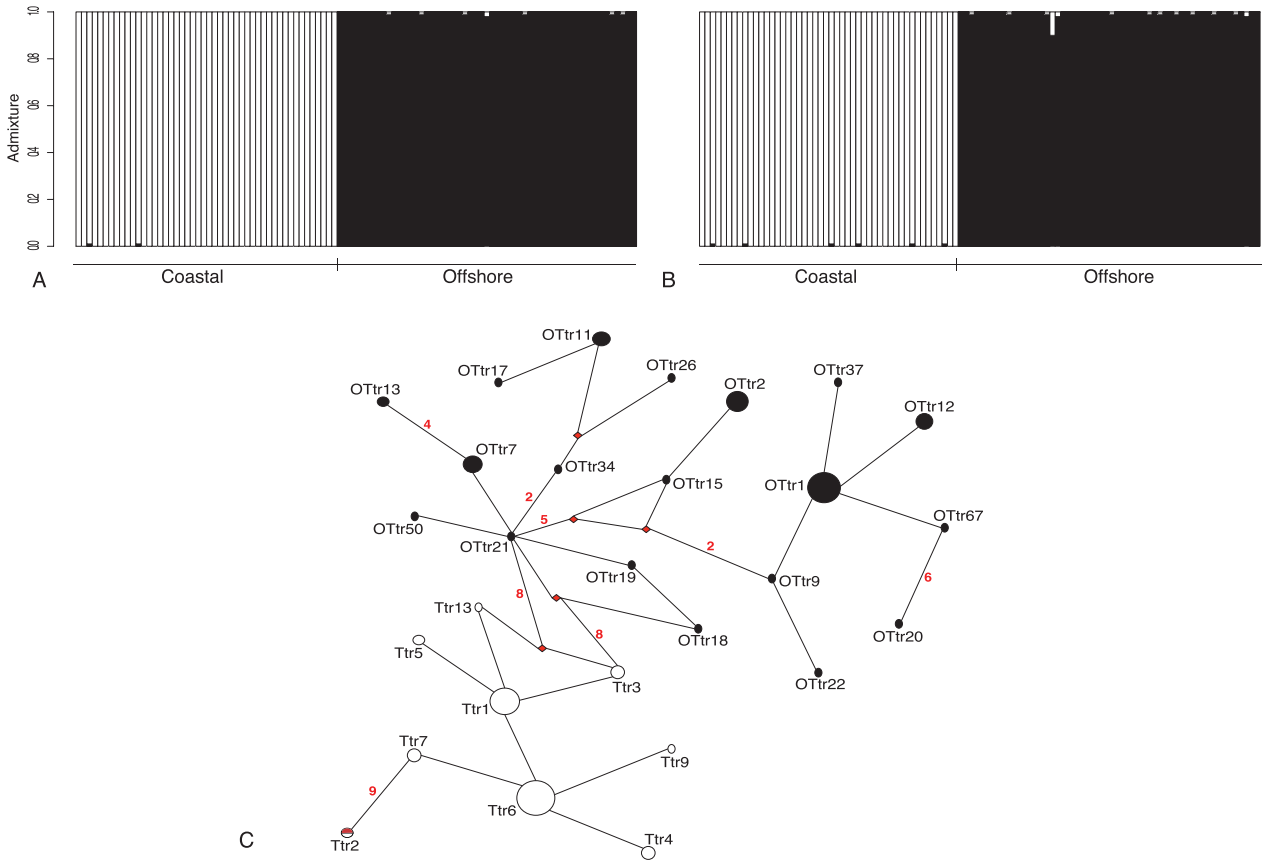

Figure 4. A, B, genetic clustering and relationship of bottlenose dolphins of the western North Atlantic. Membership probabilities of bottlenose dolphins in the western North Atlantic were based on 19 nuclear microsatellite loci and inferred using TESS (A) and STRUCTURE (B). Each column represents one individual, with colours representing the proportional membership to each of the clusters: white, coastal cluster; black, offshore cluster. C, median joining network of mitochondrial DNA haplotypes of bottlenose dolphins of the western North Atlantic. Haplotypes found in samples identified as the coastal ecotype are shown in white and those identified as the offshore ecotype in black. The size of the circles is proportional to the haplotype frequency in each group. Red diamonds indicate either extinct or unsampled haplotypes. Small red numbers on the branches represent the step mutations; branches without numbers represent one step mutation. The unique heteroplasmic haplotypes were not included in this analysis owing to program limitations to deal with ambiguous bases. The haplotype (Ttr2) obtained for the holotype *Tursiops erebennus* is in red.

was observed only in the STRUCTURE results, which subdivided the offshore samples into two groups (Supporting Information, Fig. S9). However, these groups were not correlated with any obvious geographical or morphological features and probably not related to further subdivision within this ecotype.

Alignment of the 354 bp fragment of the mtDNA control region for the 115 individuals revealed 32 haplotypes (including four hpl haplotypes) defined by 37 polymorphic sites. A total of 28 of these haplotypes were previously found in common bottlenose dolphins of the wNA: nine haplotypes were detected previously in samples identified genetically as the wNA coastal ecotype, whereas 19 were found previously in samples identified genetically as the wNA offshore ecotype. The mtDNA results demonstrated congruence with both morphological and nuclear results: samples with haplotypes previously found for the coastal ecotype also had coastal morphology and clustered together in the nuclear analyses (Fig. 4; $N = 54$; but eight samples failed to amplify up to 18 microsatellite loci), whereas samples with haplotypes previously found for the offshore ecotype also had offshore morphology and clustered together in the nuclear analyses (Fig. 4; $N = 21$; but three samples failed to amplify up to 18 microsatellite loci). Furthermore, a total of 36 of the 37 biopsy samples obtained in offshore waters presented haplotypes previously found for the genetically identified offshore ecotype, whereas one sample presented a novel offshore haplotype.

The novel haplotypes found in this study were the four heteroplasmic haplotypes (9Tt169hplO, 2Tt533hpl, 4Tt172hpl and 6Tt056hpl), each found in a single individual (GenBank accession numbers MK105887–MK105890). The first three haplotypes were obtained from samples with a skull available, which were classified morphologically as an offshore and two coastal, respectively. The last haplotype was found in the specimen biopsied in offshore waters. All four specimens were also used in the nuclear analyses; samples with haplotypes 2Tt533hpl and 4Tt172hpl were classified as coastal, and samples with haplotypes 6Tt056hpl and 9Tt169hplO as offshore by the clustering analyses. No shared haplotypes were observed between the ecotypes (Fig. 4C), and three fixed differences were found between the two mtDNA clusters. Lastly, the holotype of *T. erebennus* had a haplotype (Ttr2) that was previously detected as belonging to the coastal ecotype of the wNA and also found in another sample (USNM572263) in our data set that was classified as coastal by both the morphological and nuclear analyses.

Genetic diversity in both the nuclear and mtDNA data sets was lower for the coastal ecotype than the offshore ecotype (Table 4). A total of 243 microsatellite alleles were found in this study, with 37 private alleles in the coastal cluster, 101 private alleles in the offshore cluster, and 105 alleles shared between the ecotypes. No significant inbreeding coefficients were observed (Table 4). Significant genetic differentiation ($P < 0.0001$) was observed between the ecotypes for both nuclear (with or without related individuals: $F_{ST} = 0.18$) and mtDNA (with related individuals: $F_{ST} = 0.22$; $\Phi_{ST} = 0.71$; without related individuals: $F_{ST} = 0.21$; $\Phi_{ST} = 0.71$) markers, and with high values for Nei's d_A (0.027) and diagnosability (PD = 100%) based on the mtDNA control region sequences. Lastly, extremely low levels of ongoing gene flow (based on nuclear DNA) were observed between the coastal and offshore ecotype clusters in both directions, with both confidence intervals reaching zero (Table 5).

WORLDWIDE *TURSIOPS* MORPHOLOGICAL AND GENETIC ANALYSES

The PCA using 18 cranial measurements for 316 skulls of *T. truncatus* collected in eight different oceanographic regions suggested the presence of four well-defined clusters: (1) a cluster of coastal skulls from the wNA ($N = 102$) and skulls from the northern GOMx ($N = 18$); (2) a cluster of offshore bottlenose dolphin skulls from the eastern tropical Pacific (ETP; *nuuanu* type; $N = 15$); (3) a cluster comprising coastal skulls from the wSA (*T. t. gephyreus*; $N = 75$); and (4) a cluster composed of *T. truncatus* skulls ($N = 106$), which included offshore dolphins of both wNA ($N = 45$) and wSA ($N = 25$) origin, bottlenose dolphins from the eNA ($N = 19$), eastern South Pacific ($N = 4$), California ($N = 8$), Japan ($N = 4$) and the holotype of *T. truncatus*. The first two PCs explained 83.3% of the variation among the groups (Fig. 5).

The unsupervised clustering of the worldwide data set based on DC analysis of 18 cranial measurements identified three main clusters (Supporting Information, Fig. S10): (1) a cluster of all wNA coastal samples ($N = 102$), all northern GOMx samples ($N = 18$), eight wNA offshore samples and the majority of the ETP offshore samples (*nuuanu* type; $N = 14$); (2) a cluster of the majority of the *T. t. gephyreus*-type samples of wSA ($N = 74$) and a few *T. t. truncatus*-type samples from the eNA ($N = 3$), including the holotype *T. truncatus*;

Table 5. Mean recent (BAYESASS) migration rates between the western North Atlantic clusters (with and without the related individuals), with respective 95% confidence interval, inferred using microsatellite data

From/to	Coastal (95% confidence interval)	Offshore (95% confidence interval)
Coastal	0.993 (0.98–1.0)	0.006 (0.0–0.02)
Offshore	0.007 (0.0–0.02)	0.994 (0.98–1.0)

The migration rates were estimated as the proportion of individuals that migrate from one cluster to the other per generation. Migration rates were the same with and without related individuals.

Table 4. Nuclear (microsatellites) and mitochondrial DNA diversities for each western North Atlantic ecotype

Microsatellites								Mitochondrial DNA			
Cluster	*N*	NA	PA	F_{IS} (*P*)	H_O (SD)	H_E (SD)	AR (SD)	*N**	*H* (Hpl)	PS†	*h* (SD)†	π (SD)†
Coastal	48	142	37	0.035 (0.07)	0.642 (0.142)	0.666 (0.14)	7.449 (4.051)	56	11 (2)	15	0.702 (0.051)	0.004 (0.003)
Offshore	56	206	101	−0.008 (0.72)	0.820 (0.072)	0.815 (0.072)	10.505 (3.61)	59	21 (2)	23	0.855 (0.035)	0.018 (0.01)

*Total number considering the samples with heteroplasmic haplotypes ($N = 4$).
†The samples with heteroplasmic haplotypes ($N = 4$) were not used in these statistical analyses.
Abbreviations: AR, mean allelic richness; F_{IS}, inbreeding coefficient; *h*, haplotype diversity; *H*, total number of haplotypes; H_E, mean expected heterozygosity; H_O, mean observed heterozygosity; Hpl, total number of heteroplasmic haplotypes; *N*, number of individuals; NA, total number of alleles; *P*, F_{IS} *P*-value; PA, total number of private alleles; PS, total number of polymorphic sites; SD, standard deviation; π, nucleotide diversity.

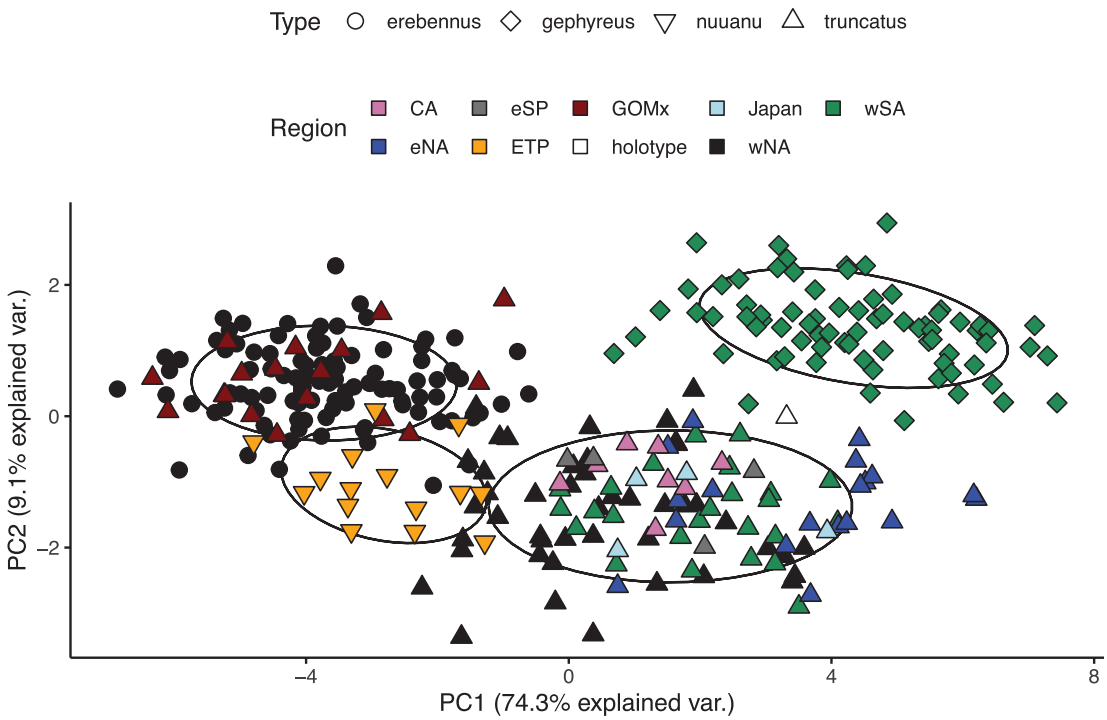

Figure 5. Worldwide morphological analyses of bottlenose dolphins. Scatter plot of the principal component 1 (PC1) and 2 (PC2) scores from the analysis of 18 skull measurements and 316 bottlenose dolphin skulls. Ellipses correspond to the 95% confidence interval. Samples are differentiated by type classification and geographical region. The holotype *Tursiops truncatus* is represented by an open triangle.

and (3) a cluster formed by all the other *T. truncatus*-type samples ($N = 95$), one *T. gephyreus*-type sample and one ETP offshore sample. Overall, these DC results showed general congruence with the type assignments and the visually identified clusters on the PCA plot (see previous paragraph). Differences in the classifications based on DC results could be attributable to similarities in skull sizes among individuals of different types. For example, despite inhabiting different oceanographic regions, ETP offshore samples (*nuuanu* type) and wNA coastal samples were clustered together by DC, possibly because of their small skull sizes – they are among the smallest bottlenose dolphins (see Table 6).

Interestingly, both PCA and DC clusters placed the northern GOMx skulls among the wNA coastal samples. These GOMx skulls also presented coastal characteristics following our a priori assignment using the five qualitative variables. Furthermore, 12 of the 18 GOMx samples had both skull and genetic information and exhibited four mtDNA haplotypes: three observed only in the GOMx data set (Ttr16, GTtr30 and GTtr45) and one haplotype (Ttr2) that was also observed in the wNA coastal data set.

The maximum likelihood analysis of the mtDNA control region alignment (311 bp) indicated that the wNA offshore samples group together with common bottlenose dolphins found worldwide (SH-aLRT: 88.2%; UFBoot: 93%) and not with coastal bottlenose dolphins of the wNA, GOMx and those identified as 'coastal' in the Bahamas and the Caribbean Sea (Fig. 6; Supporting Information, Fig. S11; Table S7). Almost all wNA coastal haplotypes grouped together in a clade (SH-aLRT: 89.6%; UFBoot: 99%) that also included two haplotypes, one found in the north of Cuba (TtruCARQ) and one from the northern Bahamas (HapGFc52) (for more information on these haplotypes, see Supporting Information, Table S7), whereas most of the 'coastal' haplotypes of the Caribbean Sea formed a second clade with the coastal GOMx samples (SH-aLRT: 86.6%; UFBoot: 87%). This clade included the coastal haplotype (Ttr2), which was shared between the GOMx and wNA and was also found in the holotype *T. erebennus* (SH-aLRT: 86.6%; UFBoot: 87%). Some (but not all) haplotypes found in Ecuador grouped together and were separated from all other *T. truncatus* samples (SH-aLRT: 92.6%; UFBoot: 98%). This clade was composed of six haplotypes: four were found in the estuarine waters of the Gulf of Guayaquil (Ecuador), one was outside the Gulf, and one was found exclusively in Peruvian

Table 6. Comparisons of condylobasal lengths, reported maximum total external body length and total number of vertebrae between the coastal ecotype of the western North Atlantic (*Tursiops erebennus*) and different ecotypes and subspecies of common bottlenose dolphins (*Tursiops truncatus*) from different ocean basins

Ocean basin	Taxonomic unit	CBL (mm)	*N*	TL (cm)	*N*	VC	*N*	Reference
Western North Atlantic	*T. erebennus* (coa)	426–510	102	286	99	59–61	21	This study
	T. truncatus (off)	466–550	45	398	43	62–65	20	
Western South Atlantic	*T. t. gephyreus* (coa)	533–609	70	366	49	57–59	17	Costa *et al.* (2016)
	T. t. truncatus (off)	495–567	30	310	14	62–68	18	
Eastern North Pacific	*T. truncatus* (coa)	471–548	29	333	17	NA	NA	Perrin & Reilly (1984);
	T. truncatus (off)	479–570	12	310	14	NA	NA	Perrin *et al.* (2011)
Eastern South Pacific	*T. truncatus* (coa)	507–542	4	308	15	NA	NA	Van Waerebeek *et al.*
	T. truncatus (off)	494–542	15	305	33	NA	NA	(1990)
Eastern North Atlantic	*T. truncatus* (coa)	NA	NA	340	12	NA	NA	Louis *et al.* (2014)
	T. truncatus (off)	NA	NA	358	27	NA	NA	
Black Sea	*T. t. ponticus*	425–467	27	244	28	NA	NA	Viaud-Martinez *et al.* (2008)
Eastern Tropical Pacific	*T. t. nuuanu**	423–512	29	275	27	NA	NA	A. P. B. Costa, F. I. Archer, P. E. Rosel, & W. F. Perrin, unpublished data

*Possible common bottlenose dolphin subspecies for the Eastern Tropical Pacific.
Abbreviations: CBL, condylobasal length; coa, coastal ecotype; *N*, number of samples; NA, not applicable; off, offshore ecotype; TL, reported maximum total external body length; VC, total number of vertebrae.

waters (see Supporting Information, Table S7). *Tursiops aduncus* (Ehrenberg, 1832) samples were split into two groups: one composed of haplotypes found in coastal waters of China/Taiwan and Australia and one haplotype from Bangladesh, and the other composed of the remaining haplotypes from Bangladesh and those from African waters, including the holotype of *T. aduncus* (Fig. 6; Supporting Information, Fig. S11), which was collected in the Red Sea (cf. Perrin *et al.*, 2007).

The alignment of the worldwide samples revealed the presence of one fixed difference at position 89 (T) between wNA coastal and all haplotypes, except the coastal samples of the GOMx, Bahamas and Caribbean Sea. This alignment also revealed that the other two fixed differences observed between the wNA ecotypes (see results above) were not exclusive to the wNA (i.e. bottlenose dolphins elsewhere also had the same nucleotide substitutions).

DISCUSSION

Morphological and genetic data distinguish the wNA ecotypes

We observed diagnostic differences in skull size and shape between coastal and offshore ecotypes of bottlenose dolphins in the wNA. In combination with differences in the vertebral column and their genetic differentiation, these lines of evidence support the hypothesis that the two ecotypes are distinct evolutionary lineages (cf. Kingston & Rosel, 2004), with ecological factors strongly influencing their evolutionary divergence.

Some of the differences between the two ecotypes in the wNA are likely to be associated with distinct feeding ecologies and habitat use. For example, differences in the width of the internal nares in dolphins have previously been proposed to indicate distinct air exchange and sound production capabilities stemming from differential habitat and prey preferences (Perrin, 1975; Perrin *et al.*, 2011). Differential prey preferences have been suggested for the wNA ecotypes (Mead & Potter, 1995): analyses of stomach contents indicated that coastal dolphins ($N = 117$) feed mainly on small to large nearshore sciaenid fishes (e.g. weakfish, Atlantic croaker, spot and American silver perch), whereas small mesopelagic fishes of the family Myctophidae and squids were found in offshore dolphins ($N = 18$). Likewise, Walker *et al.* (1999) suggested that the amount of scarring of the skull because of the parasitic nematode *Crassicauda* sp. is related to differences in diet; in our data set, almost half of the offshore skulls exhibited *Crassicauda* scars, whereas only two of the 102 coastal skulls exhibited such scars, reinforcing the suggestion of different feeding ecologies. Finally, Louis *et al.* (2021) identified several genes of ecological relevance under parallel evolution driven by habitat specialization in bottlenose dolphin ecotypes, including some that might be associated with differential diet in coastal and offshore dolphins. Thus, there is a weight of evidence supporting the hypothesis of divergence in cranial and genetic traits owing to ecological diversification.

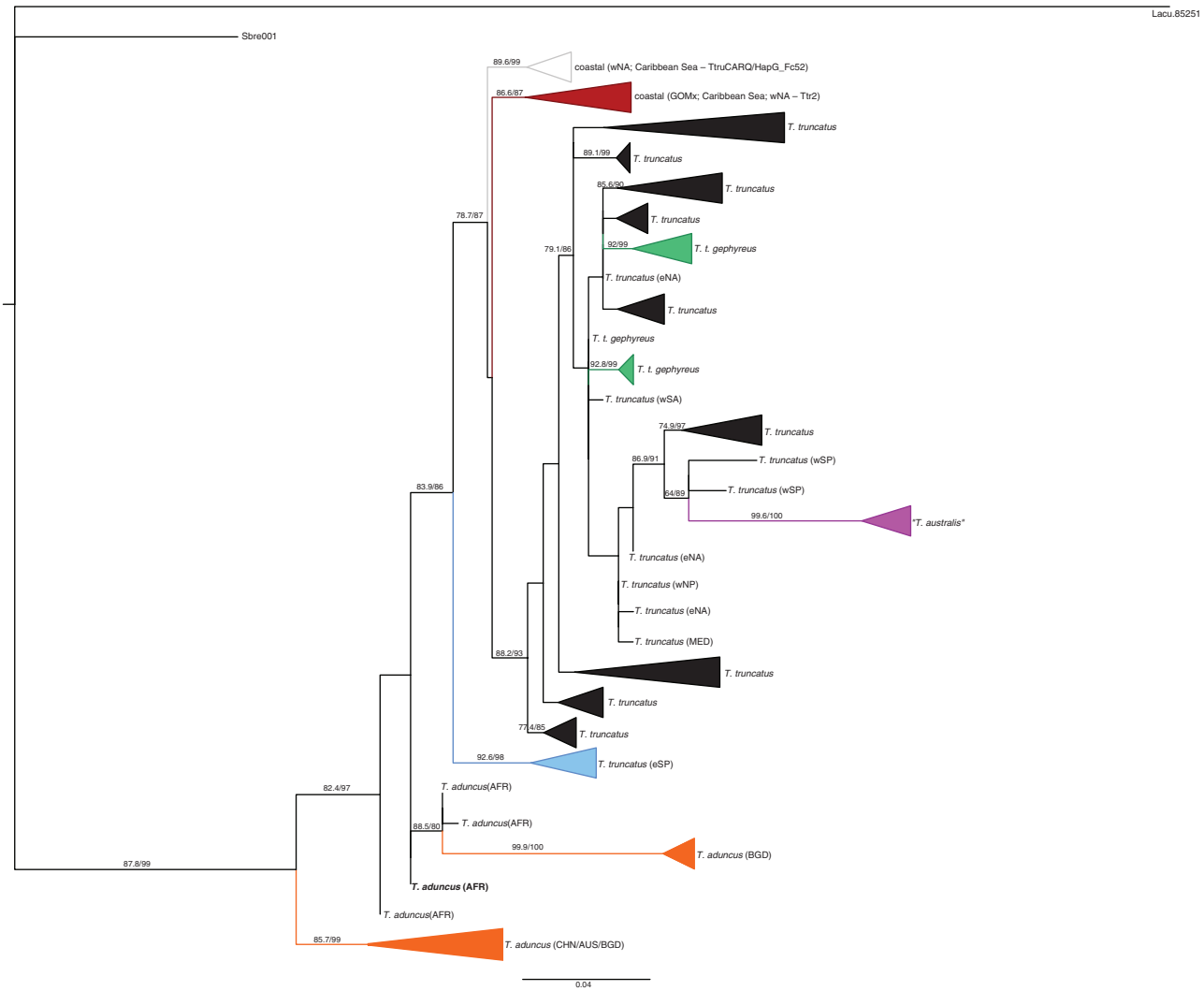

Figure 6. Compressed phylogenetic tree of bottlenose dolphins based on maximum likelihood. For sample information and the full tree, see the Supporting Information (Table S7; Fig. S11, respectively). The clade formed by seven haplotypes from this study found as the wNA coastal ecotype (and two GenBank haplotypes of the Bahamas and Cuba, respectively) is coloured in white, whereas the clade composed of three coastal haplotypes of the Gulf of Mexico, 15 of the Bahamas and Caribbean Sea, and Ttr2 (wNA coastal haplotype; *Tursiops erebennus* haplotype; GOMx coastal haplotype) is coloured in red. Most the haplotypes forming the *Tursiops truncatus* offshore clade (N = 192; including haplotypes from the present study found in the wNA offshore ecotype, in addition to GenBank haplotypes found in *T. truncatus* worldwide) are coloured in black. Highlighted inside the offshore clade are the haplotypes found in *T. t. gephyreus* (green) and '*Tursiops australis*' (purple). The clade composed of coastal *T. truncatus* from Ecuador and Peru is coloured in light blue, whereas *Tursiops aduncus* clades are coloured in orange (one clade composed of haplotypes from Bangladesh/African waters and another of haplotypes from Chinese/Australian waters and one haplotype found in Bangladesh). The haplotype found in the holotype *T. aduncus* is shown in bold. Bootstrap values (UFBoot) cut-off ≥ 80, because UFBoot achieves more unbiased support values. Shimodaira–Hasegawa-like approximate likelihood ratio test (SH-aLRT; first value) and UFBoot (second value) bootstrap values are represented on the tree branches (see also Supporting Information, Fig. S11). Abbreviations: AFR, western Indian Ocean–African coast; AUS, Australian coast; BGD, Bangladeshi coast; CHN, Chinese coast; eNA, eastern North Atlantic; eSP, eastern South Pacific; MED, Mediterranean Sea; wNA, western North Atlantic; wNP, western North Pacific; wSA, western South Atlantic; wSP, western South Pacific.

Analysis of the vertebral column of the two ecotypes in the wNA also produced two well-differentiated groups consistent with the results of the cranial analyses. Offshore dolphins in the wNA had a higher vertebral count than the coastal ecotype, but a similar vertebral count to the offshore

ecotype in the wSA (see Costa *et al.*, 2016). The total number of vertebrae in the coastal dolphins of the wNA and wSA is also similar, despite their considerable difference in total body length (Table 6). Marchesi *et al.* (2017) hypothesized that differences in vertebral column count and vertebral shape are associated with the occupied habitat. A greater number of vertebrae, especially in the lumbar region of the vertebral column, provides increased skeletal support for muscle insertions, thereby increasing vertebral column stability. More stable columns appear to be associated with the performance of high-speed manoeuvres, a characteristic of oceanic dolphins, whereas higher vertebral flexibility allows slower and more precise manoeuvres for dolphins inhabiting areas of higher complexity, such as coastal and estuarine waters (Marchesi *et al.*, 2017). The differences in the vertebral counts of the coastal and offshore ecotypes in the wNA are consistent with the patterns identified by Marchesi *et al.* (2017), further reinforcing that the two ecotypes have distinct ecological niche preferences.

Interestingly, although Costa *et al.* (2016) also found more vertebrae in the offshore vs. coastal subspecies of the wSA, the wSA offshore animals are significantly smaller than their wSA coastal counterparts, albeit still larger than the wNA coastal dolphins. In Californian waters, offshore dolphins are also smaller than coastal dolphins (Perrin *et al.*, 2011). This is the reverse of what is seen in the wNA: the coastal ecotype in the wNA is significantly smaller in body size and skull size than the offshore ecotype and the holotype *T. truncatus* (CBL, 545 mm). In fact, the coastal ecotype of the wNA has one of the smallest sizes of any measured bottlenose dolphin ecotype, possibly larger only than the Black Sea subspecies *T. t. ponticus* (Table 6).

Genetic analyses support the morphological data indicating that the wNA coastal dolphins are a unique evolutionary lineage. Samples with coastal skull morphology exhibited a unique genetic profile at both nuclear and mtDNA markers, whereas samples with offshore skull morphology presented genetic profiles similar to offshore dolphin populations elsewhere. The offshore ecotype was more genetically diverse than the coastal ecotype, a characteristic also reported previously for the wNA and elsewhere (Natoli *et al.*, 2004; Rosel *et al.*, 2009; Louis *et al.*, 2014; Costa *et al.*, 2021). No shared haplotypes and three fixed differences were found in the control region between the wNA ecotypes (when examining only the wNA data set). There is no evidence of admixture between the two ecotypes in the wNA based on the nuclear microsatellite data, and estimates of recent migration rates between these ecotypes (based on nuclear data) were extremely low and included zero in the confidence intervals (Table 5) despite the parapatric, and in some places sympatric, distribution of the ecotypes (Torres *et al.*, 2003; Hayes *et al.*, 2017). Estimates of genetic divergence based on the mtDNA, Nei's d_A (0.027) and diagnosability (PD 100%), are as high as those seen between other recognized species of cetaceans (Rosel *et al.*, 2017; Taylor *et al.*, 2017a) and agree with previous results using amplified fragment length polymorphism (AFLP) markers (Kingston & Rosel, 2004).

Phylogenetic analysis of the shorter mtDNA control region sequences separated the wNA coastal ecotype from all other *Tursiops* populations and grouped the parapatric wNA offshore ecotype in a large clade with other bottlenose dolphins worldwide (Fig. 6; Supporting Information, Fig. S11). No control region haplotypes identified in wNA coastal dolphins have been found anywhere else outside the wNA, besides the northern GOMx (Rosel *et al.*, 2009; present study) and potentially one haplotype identified from the northern Bahamas (Parsons *et al.*, 2006). In contrast, previous studies (in congruence with our results) have identified mtDNA control region haplotypes shared between wNA offshore dolphins and bottlenose dolphins from many other oceanographic regions (Hoelzel *et al.*, 1998; Natoli *et al.*, 2004; Quérouil *et al.*, 2007; Tezanos-Pinto *et al.*, 2009; Louis *et al.*, 2014; Costa *et al.*, 2021), indicating that the offshore bottlenose dolphin ecotype has a broad, circumglobal distribution, representing a worldwide lineage of oceanic *T. truncatus*.

Of interest in this global control region phylogeny are the two well-supported clades of samples collected in coastal waters of the wNA, GOMx, Bahamas and Caribbean Sea. One of these two clades comprised seven of the eight haplotypes unique to samples corresponding to wNA coastal samples, one haplotype found in one individual sampled in the northern Bahamas (Parsons *et al.*, 2006) and one haplotype representing a single dolphin assigned to the northern coast of Cuba (Caballero *et al.*, 2012). Of the 125 samples collected in Caribbean waters and assigned by Caballero *et al.* (2012) to the 'coastal' form, only this one from north of Cuba grouped within our wNA clade. The origin of this sample is not clear, because it might have been an animal sampled in captivity whose source is unknown. The second clade comprised 18 haplotypes found in the GOMx, including dolphins that grouped with wNA skulls in the morphological analysis (Fig. 5), the Bahamas and Caribbean (Parsons *et al.*, 2006; Caballero *et al.*, 2012; present study) and one haplotype (Ttr2) found in the wNA coastal ecotype and in coastal dolphins of the GOMx (present study). It is interesting that the mtDNA data indicate a strong separation between coastal animals from the wNA and those from the GOMx, whereas skull morphometrics indicate overlap of dolphins from these locations. Further work is needed to understand the relationship between these two clades of coastal-type animals,

which in turn will help to delineate the range of the unique wNA coastal ecotype.

Evolutionary distinctiveness of the wNA coastal ecotype

The distinctiveness of the wNA coastal ecotype has also been placed in the broader evolutionary context of the evolution of the genus *Tursiops*. Moura *et al.* (2013) analysed whole mitochondrial genomes (mitogenomes) and demonstrated that the coastal ecotype in the wNA formed a well-supported clade that was first to diverge from the rest of the *T. truncatus* lineage. These results also revealed that the currently recognized Black Sea bottlenose dolphin subspecies (*T. t. ponticus*) is less divergent from the *T. truncatus* lineage than are the wNA coastal dolphins (Moura *et al.*, 2013). Analyses based on nuclear markers corroborate the mitochondrial data, revealing significant divergence between the two ecotypes in the wNA. A nuclear phylogenomic analysis based on RAD-Seq data placed the wNA coastal ecotype sister to all other *T. truncatus* samples, suggesting that it diverged first, before the diversification of the *T. truncatus* lineage (Moura *et al.*, 2020). The Black Sea bottlenose dolphin subspecies (*T. t. ponticus*) was again less divergent from the *T. truncatus* lineage than the wNA coastal dolphins based on these nuclear genomic data (Moura *et al.*, 2020). Finally, results based on whole genome sequencing revealed that the offshore bottlenose dolphins of the North Atlantic (western and eastern) and eastern North Pacific form a panmictic population, whereas the coastal ecotypes of each of these oceanographic regions represent distinct populations, with some level of parallel evolution driven by ecological niche specialization (Louis *et al.*, 2021).

It is noteworthy that Louis *et al.* (2021) indicated some level of admixture between offshore and coastal dolphins in the eastern North Pacific and also between the two ecotypes in the eastern North Atlantic but found no evidence of introgression between the two ecotypes in the wNA (showing similarities with our microsatellite results). Louis *et al.* (2021) also suggested that the coastal dolphins of the wNA were the first to diverge from the ancestral offshore population. The split between the two ecotypes in the wNA was estimated at ~80 000 yr BP based on the whole genome sequences (Louis *et al.*, 2021). Interestingly, a similar time (100 000 yr BP) was estimated since the divergence of the two recognized finless porpoise species, *Neophocaena phocaenoides* (G. Cuvier, 1829) and *Neophocaena asiaeorientalis* (Pilleri & Gihr, 1972) (Zhou *et al.*, 2018).

Thus, all the genomic findings, both nuclear and mitochondrial, point to the wNA coastal ecotype being the oldest lineage to branch out of the *T. truncatus* lineage (Moura *et al.*, 2013, 2020; Louis *et al.*, 2021). Together, these results strongly indicate that the wNA coastal ecotype is a separate evolutionary lineage, divergent from the wNA offshore ecotype and all other bottlenose dolphins worldwide.

A new taxonomic unit: the wNA coastal ecotype

A robust argument for species delimitation should use multiple, independent lines of evidence indicating evolutionary distinctiveness, with congruence between the different types of data signalling strong support for species designation (Reeves *et al.*, 2004; Padial *et al.*, 2010; Schlick-Steiner *et al.*, 2010; Yeates *et al.*, 2011; Taylor *et al.* 2017a). Taylor *et al.* (2017a) also promoted multiple independent lines of evidence and provided guidelines and standards for delimiting cetacean species. They concluded, based on analyses of mtDNA, that species-level status is warranted if diagnosability equals 100% and Nei's (1987) measure of genetic divergence, $d_A > 0.02$. Furthermore, the second line of evidence must be able to rule out male-mediated gene flow and also meet species definitions (Taylor *et al.*, 2017a).

We detected 100% diagnosability of the wNA coastal ecotype in both morphological and genetic data. Our morphological findings revealed that the coastal dolphins in the wNA are one of the smallest forms of bottlenose dolphins based on both body size and skull size, with a low number of vertebrae (59–61 vertebrae) and distinct cranial features and skull shape. Additional lines of evidence, such as phylogenomic (Moura *et al.*, 2013, 2020), distribution (Torres *et al.*, 2003; Waring *et al.*, 2009; Hayes *et al.*, 2017), haematological profile (Duffield *et al.*, 1983), ecological specialization (prey, parasite loads; Mead & Potter, 1990, 1995) and selected genes (Louis *et al.* 2021), all support species-level divergence. Furthermore, the results ($d_A = 0.027$; PD = 100%) obtained for the two recommended quantitative standards for delimiting species and subspecies of cetaceans based on mtDNA sequences follow the thresholds consistent with species-level divergence (Taylor *et al.*, 2017a). Taken together, these accumulative and congruent lines of evidence strongly indicate that the wNA coastal ecotype warrants species status.

In the wNA, two species of *Tursiops* have been described previously but are synonymized with *T. truncatus*: *T. erebennus* and *T. subridens*, which were collected in the coastal waters of the Delaware River and Chesapeake Bay, respectively. Our holotype assignment analyses demonstrated that the coastal ecotype in the wNA is equivalent to the type specimens of both these two previously described species. Given that Cope's (1865) description pre-dates that of True (1884), the *erebennus* name has priority. Thus, we recommend the resurrection of the name *Tursiops erebennus* for the coastal ecotype in the wNA.

Conclusion

We used an integrative approach to evaluate comprehensively the taxonomic status of the previously recognized common bottlenose dolphin ecotypes (coastal and offshore) in the wNA. We integrated morphological and genetic analyses applied to a majority of the same individual specimens. Our findings reaffirmed the differentiation between the wNA ecotypes. We detected diagnosability in skull and vertebral morphologies and high nucleotide divergence and diagnosability, no shared haplotypes, presence of fixed substitutions, negligible gene flow and marked phylogenetic differentiation. Additional genome-wide data from nuclear RADseq (Moura *et al.*, 2020) and whole genome sequencing (Louis *et al.*, 2021) further support divergence of the wNA coastal ecotype. The cumulative and congruent lines of evidence support species delimitation: the wNA coastal ecotype is restricted to coastal and estuarine waters of the wNA, whereas the wNA offshore group is part of a worldwide species (*T. truncatus*). The relationship of the wNA coastal ecotype to coastal dolphins of the GOMx and Caribbean Sea bears further study.

TAXONOMIC TREATMENT

Based on the morphological and genetic characters reviewed above, we propose *Tursiops erebennus* (Cope, 1865) to be a valid taxon removed from synonymy with *T. truncatus*.

Order Cetartiodactyla Montgelard, Catzefils & Douzery, 1997

Cetacea Brisson, 1762

Family Delphinidae Gray, 1821

Genus *Tursiops* Gervais, 1855

Tursiops erebennus (Cope, 1865)

Synonymy: Delphinus erebennus Cope, 1865; *Tursiops subridens* True, 1884.

Suggested common name: Tamanend's bottlenose dolphin.

Etymology: The generic name, *Tursiops*, derived from Latin *Tursio* (Latin), a dolphin-like fish in Pliny's *Natural History*, originally from *thyrsiōn* (Greek). The suffix *-ops* (Greek) is a reference to the face or appearance. For the species epithet, *erebennus*, Cope did not provide an etymology, but he mentioned an apparently darker coloration (Cope, 1865: 281). Thus, his use of *erebennus* might reference Erebus or Erebos, (Ἔρεβος) a Greek mythological primordial deity representing deep darkness or shadow. The English common name references Chief Tamanend (1628–1701) of the Turtle Clan of the Nanticoke Lenni-Lenape Tribal Nation. Chief Tamanend ('The Affable') was known for his wisdom and peaceful nature, and he signed a series of peace treaties with William Penn (founder of the Province of Pennsylvania), starting in 1683. The Nanticoke Lenni-Lenape Tribal Nation is formed by the descendants of the Lenni-Lenape Tribe and the Nanticoke Tribe, the original people to inhabit the lands between south-eastern New York and Delmarva Peninsula, including all of New Jersey, eastern Pennsylvania and Delaware Bay, the region where the holotype of *Tursiops erebennus* was found. This common name was chosen in consultation with representatives of the Nanticoke Lenni-Lenape Tribal Nation.

Holotype and type locality: Physically mature (incomplete) postcranial skeleton (Fig. 7) of unknown sex (≥ 228.6 cm) in the Academy of Natural Sciences of Drexel University (deposited under the museum number *ANSP 3020*), collected by S. B. Howell (collector). The specimen was obtained from a fisherman's seine net at the Red Bank, a community in the West Deptford Township (NJ, USA), along the Delaware River, to the east of Philadelphia (PA, USA). Vertebral formula: $C_7 + T_{12} + L_{14} + Ca_{14+}$. Mitochondrial DNA control region haplotype (354 bp): Ttr2 (GenBank accession number: OM540927).

Diagnosis: The skulls of *T. erebennus* can be differentiated from *T. truncatus* (offshore ecotype in the western North Atlantic) using the following five morphological features together. As observed from the left lateral view (Supporting Information, Fig. S1C): (1) cranial vertex elevated (anterior end of the nasals at slightly higher height than the other components of the cranial vertex); (2) shorter lacrimal, with its anterior end more flat (square shaped) and ending before the anterior end of the ascending process of the maxilla (usually, the latter is fully covering the anterior end of the lacrimal, which ends at almost the same height as the preorbital process of the frontal); and (3) straight (non-convex) pharyngeal crest. As observed from the ventral view (Supporting Information, Fig. S1D): (4) intermediate to narrower vomer when compared with the posterior process of the pterygoids; and (5) the posterior border of the pterygoid hamuli is more in an acute angle to the sagittal plane of the skull. *Tursiops erebennus* specimens can also be differentiated from *T. truncatus* specimens based on molecular genetic characters: one fixed difference was found in the mtDNA control region between the species (based on a fragment of

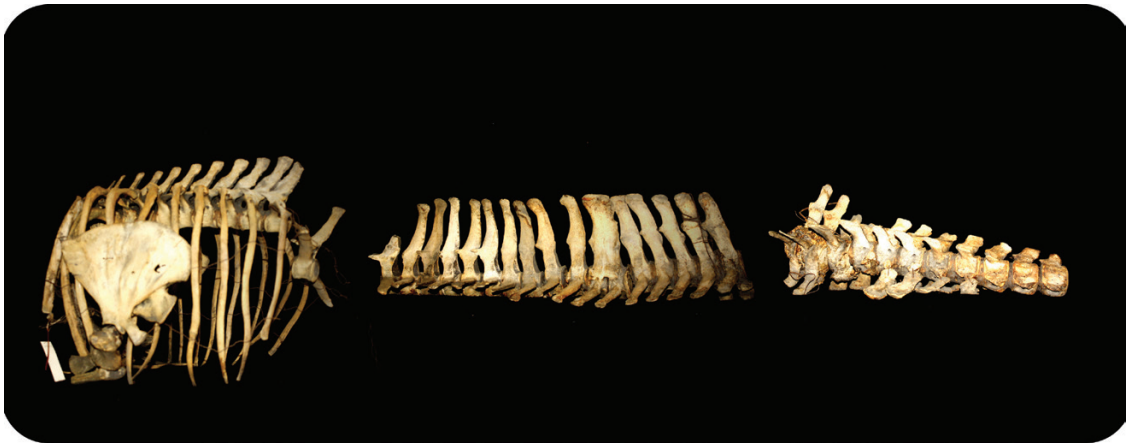

Figure 7. Assembled portions of the postcranial skeleton of the holotype *Tursiops erebennus* (Cope, 1865) deposited in the Academy of Natural Sciences of Drexel University (museum number *ANSP 3020*).

311 bp and 249 mtDNA control region haplotype sequences).

Redescription: This is a small species of bottlenose dolphin, with a known maximum total body length of 286 cm. When considering only physically mature animals based on the vertebral column ($N = 13$), we found a known minimum total adult body length of 232 cm and a mean of 256 cm for the species. It can be differentiated from *T. truncatus* based on skull morphometrics (Mead & Potter, 1995; Toledo, 2013; present study), vertebral column morphology (present study), several genetic markers (Hoelzel *et al.*, 1998; Kingston & Rosel, 2004; Rosel *et al.*, 2009; present study), body length (Mead & Potter, 1995; present study), distribution (Torres *et al.*, 2003; Rosel *et al.*, 2009; Waring *et al.*, 2009; Hayes *et al.*, 2017), parasite load (Mead & Potter, 1990), food habits (Mead & Potter, 1995), haematological profile (Duffield *et al.*, 1983) and, possibly, colour pattern (Wells & Scott, 1999). Based on our data set, the condylobasal length in physically mature skulls ranges from 426 to 510 mm, but it is possible that a larger sample size might show individuals outside this range. Physically mature skulls have a relatively short (based on our data set: 226.38–278.74 mm) and narrow (based on our data set: 65.87–86.43 mm) rostrum and narrow internal nares (based on our data set: 56.11–72.77 mm). The vertebral formula, based on 21 individuals, is $C_7 + T_{12} + L_{14–15} + Ca_{26–28} = 59–61$. It is uncommon to find scars of *Crassicauda* sp. in the skulls. There are, on average, 23 or 24 alveoli/teeth in each of the tooth rows. There is sexual dimorphism in this lineage based on traditional morphometric analysis of the skulls (with males usually being larger than females based on the skull data set) but not detected with geometric morphometrics.

Distribution: Tursiops erebennus is distributed continuously along the western North Atlantic coast from New York to the east coast of the Florida Peninsula, inhabiting nearshore coastal and estuarine waters (Rosel *et al.*, 2009; Waring *et al.*, 2009). The extent of the distribution of this species further offshore on the continental shelf of the wNA and in other areas, such as the Gulf of Mexico, Bahamas and the Caribbean, is unknown. However, to date 'coastal'-form dolphins from the Caribbean Sea have not shared haplotypes with *T. erebennus*, with a potential exception for only one dolphin from the northern Bahamas. Instead, they are placed in a separate, well-supported clade in the mtDNA control region phylogeny, suggesting some degree of divergence from *T. erebennus*. Given this apparent genetic divergence between the wNA coastal and Gulf of Mexico and Caribbean coastal animals, we recommend, at this time, that the south-east coast of Florida should be considered the southern limit for the distribution of *T. erebennus*. Further investigation is needed to resolve the relationship between these two clades, which in turn will clarify the distribution of *T. erebennus*.

ACKNOWLEDGEMENTS

We thank Charley Potter, James Mead, John Ososky, Darrin Lunde, Kristofer Helgen and Nicole Edmison (Smithsonian National Museum of Natural History) for their help and access to samples (skulls, vertebral columns and tissue samples), including

the syntypes of *T. subridens* (*USNM A 16504* and *USNM A 16505*) and the use of the MicroScribe at the Smithsonian Institution's Museum Support Center. Our acknowledgements are also extended to Dave Cicimurri (South Carolina State Museum), Jacob Esselstyn (Louisiana State University) and Zena Timmons and Jerry Herman (National Museum of Scotland) for further access to specimens for the morphological analyses, and we are very grateful to Ned Gilmore (Academy of Natural Sciences of Drexel University) and to Richard Sabin (Natural History Museum, London) for their help with access to the holotypes of *T. erebennus* (*ANSP 3020*) and *T. truncatus* (*NHMUK 353a*), respectively. We also thank Aleta Hohn and the NOAA Fisheries Beaufort Laboratory marine mammal stranding responders for their response to and sample collection from bottlenose dolphin strandings in North Carolina; Wayne Hoggard (NOAA Fisheries SEFSC) and John Nicolas (NOAA Fisheries NEFSC), who collected the majority of the biopsy samples from offshore waters during NOAA Fisheries cruises in the western North Atlantic; and D. Waples (Duke University), who provided two biopsy samples from the mid-Atlantic. Furthermore, acknowledgements are extended to the stranding responders from Dauphin Island Sea Lab, Louisiana Department of Wildlife and Fisheries, Institute for Marine Mammals Studies (Mississippi) and Audubon Aquarium of the Americas for all the hard work they put into collecting specimens of bottlenose dolphins that stranded in the northern Gulf of Mexico during the *Deepwater Horizon* incident. We also appreciate the help provided by Jenny Litz (NOAA Fisheries SEFSC, Miami) and Keith Mullin, Kevin Barry, Errol Ronje, Carrie Sinclair, Lauren Noble and Melissa Cook (NOAA Fisheries SEFSC, Pascagoula) with the acquisition and/or cleaning of the skulls of these Gulf of Mexico samples. We are also grateful to Thomas Jefferson (NOAA Fisheries SWFSC) for his valuable help with the nomenclatural taxonomy, Nicole Vollmer (NOAA Fisheries SEFSC, Lafayette) for her assistance with sampling access in previous years, Kory Evans (Rice University) for assistance with geometric morphometric analyses, and Scott France, Joe Neigel, James Albert (University of Louisiana at Lafayette), John Wang (Cetasia Research Group) and an anonymous reviewer for valuable comments in the manuscript. We are extremely grateful for the valuable input and time of Danielle Cranmer and the council members of the Nanticoke Lenni-Lenape Tribal Nation, for advice and consultation on a common name for the species *T. erebennus*. We also thank all the Brazilian researchers and their teams that provided access to skull samples from Brazil to A.P.B.C. in previous years: Paulo C. Simões-Lopes (Laboratório de Mamíferos Aquáticos at Universidade Federal de Santa Catarina; LAMAQ-UFSC), Eduardo Secchi (Laboratório de Mamíferos Marinhos e Tartarugas Marinhas at Universidade Federal de Rio Grande; EcoMega-FURG), Pedro V. Castilho (Laboratório de Zoologia at Universidade do Estado de Santa Catarina; UDESC) and Marta Cremer (Acervo Biológico Iperoba at Universidade da Região de Joinville; UNIVILLE). The scientific results and conclusions, in addition to any views or opinions expressed herein, are those of the authors and do not necessarily reflect those of NOAA or the Department of Commerce. This research was produced during A.P.B.C.'s Ph.D. at the University of Louisiana at Lafayette, with a Ph.D. scholarship provided by Coordenação e Aperfeiçoamento de Pessoal de Nível Superior (Capes Foundation). Coordenação e Aperfeiçoamento de Pessoal de Nível Superior (Capes Foundation); Grant/Award Number: 99999.010007/2013-00. Graduate Student Organization (GSO), University of Louisiana at Lafayette.

DATA AVAILABILITY

Haplotypes found in this study were deposited in GenBank under the accession numbers MK105887–MK105890 and OM540927. Additional morphological and microsatellite data sets and R scripts can be obtained upon request.

REFERENCES

Adams DC, **Collyer ML**, **Kaliontzopoulou A**, **Baken EK. 2021.** *Geomorph: software for geometric morphometric analyses. R package version 4.0*. Available at: https://cran.r-project.org/package=geomorph

Adams DC, **Nistri A. 2010.** Ontogenetic convergence and evolution of foot morphology in European cave salamanders (family: Plethodontidae). *BMC Evolutionary Biology* **10:** 216.

Agapow P-M, **Bininda-Emonds ORP**, **Crandall KA**, **Gittleman JL**, **Mace GM**, **Marshall JC**, **Purvis A. 2004.** The impact of species concept on biodiversity studies. *The Quarterly Review of Biology* **79:** 161–179.

Amos W, **Hoelzel AR. 1991.** Long-term preservation of whale skin for DNA analysis. *Reports of the International Whaling Commission, Special Issue* **13:** 99–104.

Archer FI. 2021. *rfPermute: estimate permutation p-values for Random Forest importance metrics. R package version 2.5*. Available at: https://CRAN.R-project.org/package=rfPermute

Archer FI, **Adams PE**, **Schneiders BB. 2017a.** STRATAG: an R package for manipulating, summarizing and analysing population genetic data. *Molecular Ecology Resources* **17:** 5–11.

Archer FI, **Martien KK**, **Taylor BL. 2017b.** Diagnosability of mtDNA with Random Forests: using sequence data to delimit subspecies. *Marine Mammal Science* **33:** 101–131.

Arnold TB, **Emerson JW. 2011.** Nonparametric goodness-of-fit tests for discrete null distribution. *The R Journal* **3:** 34–39.

Bandelt HJ, **Forster P**, **Röhl A. 1999.** Median-joining networks for inferring intraspecific phylogenies. *Molecular Biology and Evolution* **16:** 37–48.

Caballero S, **Islas-Villanueva V**, **Tezanos-Pinto G**, **Duchene S**, **Delgado-Estrella A**, **Sanchez-Okrucky R**, **Mignucci-Giannoni AA. 2012.** Phylogeography, genetic diversity and population structure of common bottlenose dolphins in the wider Caribbean inferred from analyses of mitochondrial DNA control region sequences and microsatellite loci: conservation and management implications. *Animal Conservation* **15:** 95–112.

Collyer ML, **Adams DC. 2018.** RRPP: an R package for fitting linear models to high-dimensional data using residual randomization. *Methods in Ecology and Evolution* **9:** 1772–1779.

Cope ED. 1865. Second contribution to a history of the Delphinidae. *Proceedings of the Academy of Natural Sciences of Philadelphia* **17:** 278–281.

Costa APB, **Fruet PF**, **Secchi ER**, **Daura-Jorge FG**, **Simões-Lopes PC**, **Di Tullio JC**, **Rosel PE. 2021.** Ecological divergence and speciation in common bottlenose dolphins in the western South Atlantic. *Journal of Evolutionary Biology* **34:** 16–32.

Costa APB, **Rosel PE**, **Daura-Jorge FG**, **Simões-Lopes PC. 2016.** Offshore and coastal common bottlenose dolphins of the western South Atlantic face-to-face: what the skull and the spine can tell us. *Marine Mammal Science* **32:** 1433–1457.

Costa APB, **Simões-Lopes PC. 2012.** Physical maturity of the vertebral column of *Tursiops truncatus* (Cetacea) from southern Brazil. *Neotropical Biology and Conservation* **7:** 2–7.

Dayrat B. 2005. Towards integrative taxonomy. *Biological Journal of the Linnean Society* **85:** 407–415.

Duffield DA, **Ridgway SH**, **Cornell LH. 1983.** Hematology distinguishes coastal and offshore forms of dolphins (*Tursiops*). *Canadian Journal of Zoology* **61:** 930–933.

Durand E, **Chen C**, **François O. 2009.** *Tess version 2.3 - reference manual*. Available at: http://membres-timc.imag.fr/Olivier.Francois/manual.pdf

Excoffier L, **Lischer HEL. 2010.** Arlequin suite ver 3.5: a new series of programs to perform population genetics analyses under Linux and Windows. *Molecular Ecology Resources* **10:** 564–567.

Fox J, **Weisberg S. 2019.** *An R companion to applied regression, 3rd edn*. Thousand Oaks, California: SAGE Publications.

Garnier-Géré P, **Chikhi L. 2013.** *Population subdivision, Hardy–Weinberg Equilibrium and the Wahlund effect*. Chichester: eLS, John Wiley & Sons.

Glaubitz JC. 2004. CONVERT: a user-friendly program to reformat diploid genotypic data for commonly used population genetic software packages. *Molecular Ecology Notes* **4:** 309–310.

Goudet J. 1995. FSTAT (version 1.2): a computer program to calculate *F*-statistics. *Journal of Heredity* **86:** 485–486.

Guindon S, **Dufayard J-F**, **Lefort V**, **Anisimova M**, **Hordijk W**, **Gacuel O. 2010.** New algorithms and methods to estimate maximum-likelihood phylogenies: assessing the performance of PhyML 3.0. *Systematic Biology* **59:** 307–321.

Guo SW, **Thompson EA. 1992.** Performing the exact test of Hardy–Weinberg proportion for multiple alleles. *Biometrics* **48:** 361–372.

Hasegawa M, **Kishino H**, **Yano T. 1985.** Dating of the human-ape splitting by molecular clock of mitochondrial DNA. *Journal of Molecular Evolution* **22:** 160–174.

Hausdorf B. 2011. Progress toward a general species concept. *Evolution; international journal of organic evolution* **65:** 923–931.

Hayes SA, **Josephson E**, **Maze-Foley K**, **Rosel PE. 2017.** US Atlantic and Gulf of Mexico marine mammal stock assessments—2016. *NOAA Technical Memorandum NMFS-NE* **241**. Available at: https://repository.library.noaa.gov/view/noaa/14864.

Hoelzel AR, **Potter CW**, **Best PB. 1998.** Genetic differentiation between parapatric 'nearshore' and 'offshore' populations of the bottlenose dolphin. *Proceedings of the Royal Society B: Biological Sciences* **265:** 1177–1183.

Holm S. 1979. A simple sequentially rejective multiple test procedure. *Scandinavian Journal of Statistics* **6:** 65–70.

Issac NJB, **Mallet J**, **Mace GM. 2004.** Taxonomic inflation: its influence on macroecology and conservation. *Trends in Ecology & Evolution* **19:** 464–469.

Jordan F, **Murphy S**, **Martinez E**, **Amiot C**, **Van Helden A**, **Stockin KA. 2015.** Criteria for assessing maturity of skulls in the common dolphin, *Delphinus* sp., from New Zealand waters. *Marine Mammal Science* **31:** 1077–1097.

Kingston SE, **Rosel PE. 2004.** Genetic differentiation among recently diverged delphinid taxa determined using AFLP markers. *Journal of Heredity* **95:** 1–10.

Knowles LL, **Carstens B. 2007.** Delimiting species without monophyletic gene trees. *Systematic Biology* **56:** 887–895.

Li CC, **Weeks DE**, **Chakravarti A. 1993.** Similarity of DNA fingerprints due to chance and relatedness. *Human Heredity* **43:** 45–52.

Liaw A, **Wiener M. 2002.** Classification and regression by randomForest. *R News* **2:** 18–22.

Louis M, **Galimberti M**, **Archer F**, **Berrow S**, **Brownlow A**, **Fallon R**, **Nykänen M**, **O'Brien J**, **Roberston KN**, **Rosel PE**, **Simon-Bouhet B**, **Wegmann D**, **Fontaine MC**, **Foote AD**, **Gaggiotti OE. 2021.** Selection on ancestral genetic variation fuels repeated ecotype formation in bottlenose dolphins. *Science Advances* **7:** eabg1245.

Louis M, **Viricel A**, **Lucas T**, **Peltier H**, **Alfonsi E**, **Berrow S**, **Brownlow A**, **Covelo P**, **Dabin W**, **Deaville R**, **De Stephanis R. 2014.** Habitat-driven population structure of bottlenose dolphins, *Tursiops truncatus*, in the North-East Atlantic. *Molecular Ecology* **23:** 857–874.

Lynch M, **Ritland K. 1999.** Estimation of pairwise relatedness with molecular markers. *Genetics* **152:** 1753–1766.

Marchesi MC, **Mora MS**, **Pimper LE**, **Crespo EA**, **Goodall RNP. 2017.** Can habitat characteristics shape vertebral morphology in dolphins? An example of two phylogenetically related species from southern South America. *Marine Mammal Science* **33:** 1126–1148.

Mead JG, **Potter CW. 1990.** Natural history of bottlenose dolphins along the central Atlantic Coast of the United States. In: Leatherwood S, Reeves RR, eds. *The bottlenose dolphin*. San Diego: Academic Press, 165–195.

Mead JG, **Potter CW. 1995.** Recognizing two populations of the bottlenose dolphin (*Tursiops truncatus*) off the Atlantic coast of North America: morphologic and ecologic considerations. *IBI Reports* **5:** 31–44.

Miller MA, **Pfeiffer W**, **Schwartz T. 2010.** Creating the CIPRES Science Gateway for inference of large phylogenetic trees. *Proceedings of the Gateway Computing Environments Workshop*. New Orleans: IEEE. Available at: http://www.phylo.org/sub_sections/portal/cite.php

Milligan BG. 2003. Maximum-likelihood estimation of relatedness. *Genetics* **163:** 1153–1167.

Minh BQ, **Nguyen MAT**, **von Haeseler A. 2013.** Ultrafast approximation for phylogenetic bootstrap. *Molecular Biology and Evolution* **30:** 1188–1195.

Moura AE, **Nielsen SC**, **Vilstrup JT**, **Moreno-Mayar JV**, **Gilbert MT**, **Gray HW**, **Natoli A**, **Möller L**, **Hoelzel AR. 2013.** Recent diversification of a marine genus (*Tursiops* spp.) tracks habitat preference and environmental change. *Systematic Biology* **62:** 865–877.

Moura AE, **Shreves K**, **Pilot M**, **Andrews KR**, **Moore DM**, **Kishida T**, **Möller L**, **Natoli A**, **Gaspari S**, **McGowen M**, **Chen I**, **Gray H**, **Gore M**, **Culloch RM**, **Kiani MS**, **Willson MS**, **Bulushi A**, **Collins T**, **Baldwin R**, **Willson A**, **Minton G**, **Ponnampalam L**, **Hoelzel AR. 2020.** Phylogenomics of the genus *Tursiops* and closely related Delphininae reveals extensive reticulation among lineages and provides inference about eco-evolutionary drivers. *Molecular Phylogenetics and Evolution* **146:** 106756.

Natoli A, **Peddemors VM**, **Hoelzel AR. 2004.** Population structure and speciation in the genus *Tursiops* based on microsatellite and mitochondrial DNA analyses. *Journal of Evolutionary Biology* **17:** 363–375.

Nei M. 1987. *Molecular evolutionary genetics*. New York: Columbia University Press.

Nei M, **Tajima F. 1981.** DNA polymorphism detectable by restriction endonucleases. *Genetics* **97:** 145–163.

Padial JM, **Miralles A**, **De la Riva I**, **Vences M. 2010.** The integrative future of taxonomy. *Frontiers in Zoology* **7:** 16.

Park SDE. 2001. *Trypanotolerance in West African cattle and the population genetic effects of selection*. Unpublished D. Phil. Thesis, University of Dublin.

Parsons KM, **Durban JW**, **Claridge DE**, **Herzing DL**, **Balcomb KC**, **Noble LR. 2006.** Population genetic structure of coastal bottlenose dolphins (*Tursiops truncatus*) in the northern Bahamas. *Marine Mammal Science* **22:** 276–298.

Pedersen TL, **Hughes S**, **Qiu X. 2017.** *densityClust: clustering by fast search and find of density peaks. R package version 0.3*. Available at: https://CRAN.R-project.org/package=densityClust

Perrin WF. 1975. *Variation of spotted and spinner porpoise (genus Stenella) in the eastern Pacific and Hawaii. Bulletin of the Scripps Institute of Oceanography, University of California, Vol. 21.* Berkeley and Los Angeles: University of California Press.

Perrin WF, Reilly SB. 1984. Reproductive parameters of dolphins and small whales of the family Delphinidae. *Report of the International Whaling Commission* **6**: 97–133.

Perrin WF, **Robertson KM**, **Van Bree PJH**, **Mead JG. 2007.** Cranial description and genetic identity of the holotype specimen of *Tursiops aduncus* (Ehrenberg, 1832). *Marine Mammal Science* **23:** 343–357.

Perrin WF, **Thieleking JL**, **Walker WA**, **Archer FI**, **Robertson KM. 2011.** Common bottlenose dolphins (*Tursiops truncatus*) in California waters: cranial differentiation of coastal and offshore ecotypes. *Marine Mammal Science* **27:** 769–792.

Pew J, **Muir PH**, **Wang J**, **Frasier TR. 2015.** related: an R package for analyzing pairwise relatedness from codominant molecular markers. *Molecular Ecology Resources* **15:** 557–561.

Posada D. 2008. jModelTest: phylogenetic model averaging. *Molecular Biology and Evolution* **25:** 1253–1256.

Pritchard JK, **Wen X**, **Falush D. 2010.** *Documentation for* structure *software: Version 2.3*. Available at: https://web.stanford.edu/group/pritchardlab/software/structure_v.2.3.1/documentation.pdf

de Queiroz K. 2007. Species concepts and species delimitation. *Systematic Biology* **56:** 879–886.

Queller DC, **Goodnight KF. 1989.** Estimating relatedness using genetic markers. *Evolution; international journal of organic evolution* **43:** 258–275.

Quérouil S, **Silva MA**, **Freitas L**, **Prieto R**, **Magalhães S**, **Dinis A**, **Alves F**, **Matos JA**, **Mendonça D**, **Hammond PS**, **Santos RS. 2007.** High gene flow in oceanic bottlenose dolphins (*Tursiops truncatus*) of the North Atlantic. *Conservation Genetics* **8:** 1405.

R Core Team. 2019. *R: a language and environment for statistical computing*. Vienna: R Foundation for Statistical Computing.

R Core Team. 2021. *R: A language and environment for statistical computing*. Vienna: R Foundation for Statistical Computing.

Rannala B. 2015. *BayesAss edition 3.0 user's manual*. Available at: https://github.com/brannala/BA3/blob/master/doc/BA3Manual.pdf

Reeves RR, **Perrin WF**, **Taylor BL**, **Baker CS**, **Mesnick SL. 2004.** Report of the workshop on shortcomings of cetacean taxonomy in relation to needs of conservation and management. *NOAA Technical Memorandum NMFS-SWFSC* 363.

Rodrigues A, **Laio A. 2014.** Clustering by fast search and find of density peaks. *Science* **344:** 1492.

Rohlf FJ. 1999. Shape statistics: Procrustes superimpositions and tangent spaces. *Journal of Classification* **16:** 197–223.

Rohlf FJ, **Slice DE. 1990.** Extensions of the Procrustes method for the optimal superimposition of landmarks. *Systematic Zoology* **39:** 40–59.

Rosel PE, **Dizon AE**, **Heyning JE. 1994.** Genetic analysis of sympatric morphotypes of common dolphins (genus *Delphinus*). *Marine Biology* **119:** 159–167.

Rosel PE, **France SC**, **Wang JY**, **Kocher TD. 1999.** Genetic structure of harbour porpoise *Phocoena phocoena* populations

in the northwest Atlantic based on mitochondrial and nuclear markers. *Molecular Ecology* **8:** S41–S54.

Rosel PE, **Hansen L**, **Hohn AA. 2009.** Restricted dispersal in a continuously distributed marine species: common bottlenose dolphins *Tursiops truncatus* in coastal waters of the western North Atlantic. *Molecular Ecology* **18:** 5030–5045.

Rosel PE, **Taylor BL**, **Hancock-Hanser BL**, **Morin PA**, **Archer FI**, **Lang AR**, **Mesnick SL**, **Pease VL**, **Perrin WF**, **Robertson KM**, **Leslie MS. 2017.** A review of molecular genetic markers and analytical approaches that have been used for delimiting marine mammal subspecies and species. *Marine Mammal Science* **33:** 56–75.

Ross GJB, **Cockcroft VG. 1990.** Comments on Australian bottlenose dolphins and the taxonomic status of *Tursiops aduncus* (Ehrenberg, 1832). In: Leatherwood S, Reeves RR, eds. *The bottlenose dolphin*. San Diego: Academic Press, 101–128.

Rousset F. 2008. GENEPOP'007: a complete re-implementation of the GENEPOP software for Windows and Linux. *Molecular Ecology Resources* **8:** 103–106.

Schlick-Steiner BC, **Steiner FM**, **Seifert B**, **Stauffer C**, **Christian E**, **Crozier RH. 2010.** Integrative taxonomy: a multisource approach to exploring biodiversity. *Annual Review of Entomology* **55:** 421–438.

Sellas AB, **Wells RS**, **Rosel PE. 2005.** Mitochondrial and nuclear DNA analyses reveal fine scale geographic structure in bottlenose dolphins (*Tursiops truncatus*) in the Gulf of Mexico. *Conservation Genetics* **6:** 715–728.

Taylor BL, **Archer FI**, **Martien KK**, **Rosel PE**, **Hancock-Hanser BL**, **Lang AR**, **Leslie MS**, **Mesnick SL**, **Morin PA**, **Pease VL**, **Perrin WF. 2017a.** Guidelines and quantitative standards to improve consistency in cetacean subspecies and species delimitation relying on molecular genetic data. *Marine Mammal Science* **33:** 132–155.

Taylor BL, **Perrin WF**, **Reeves RR**, **Rosel PE**, **Wang JY**, **Cipriano F**, **Baker CS**, **Brownell RL Jr**. **2017b.** Why we should develop guidelines and quantitative standards for using genetic data to delimit subspecies for data-poor organisms like cetaceans. *Marine Mammal Science* **33:** 12–26.

Tezanos-Pinto G, **Baker CS**, **Russell K**, **Martien K**, **Baird RW**, **Hutt A**, **Stone G**, **Mignucci-Giannoni AA**, **Caballero S**, **Endo T**, **Lavery S. 2009.** A worldwide perspective on the population structure and genetic diversity of bottlenose dolphins (*Tursiops truncatus*) in New Zealand. *Journal of Heredity* **100:** 11–24.

Toledo GAC. 2013. *Variação geográfica em crânios de golfinhos nariz-de-garrafa,* Tursiops *Gervais, 1855, no Atlântico Ocidental* [Geographic variation in the skulls of bottlenose dolphins, *Tursiops* Gervais, 1855, in the western Atlantic]. Unpublished D. Phil. Thesis, Universidade Federal da Paraíba.

Torres LG, **Rosel PE**, **D'Agrosa C**, **Read AJ. 2003.** Improving management of overlapping bottlenose dolphin ecotypes through spatial analysis and genetics. *Marine Mammal Science* **19:** 502–514.

Trifinopoulos J, **Nguyen L-T**, **von Haeseler A**, **Minh BQ. 2016.** W-IQ-TREE: a fast online phylogenetic tool for maximum likelihood analysis. *Nucleic Acids Research* **44:** W232–W235.

True FW. 1884.Catalogue of the aquatic mammals. *United States National Museum Bulletin* **27:** 623–644.

True FW. 1889. Contributions to the natural history of the cetaceans, a review of the family Delphinidae. *United States National Museum Bulletin* **36:** 1–191.

Van Oosterhout C, **Hutchinson WF**, **Wills DPM**, **Shipley P. 2004.** MICRO-CHECKER: software for identifying and correcting genotyping errors in microsatellite data. *Molecular Ecology Notes* **4:** 535–538.

Van Waerebeek K, Reyes JC, Read AJ, McKinnon JS. 1990. Preliminary observations of bottlenose dolphins from the Pacific coast of South America. In: Leatherwood S, Reeves RR, eds. *The bottlenose dolphin*. San Diego: Academic Press, 143–154.

Viaud-Martinez KA, **Brownell RL Jr**, **Komnenou A**, **Bohonak AJ. 2008.** Genetic isolation and morphological divergence of Black Sea bottlenose dolphins. *Biological Conservation* **141:** 1600–1611.

Vollmer NL, **Rosel PE. 2017.** Fine-scale population structure of common bottlenose dolphins (*Tursiops truncatus*) in offshore and coastal waters of the US Gulf of Mexico. *Marine Biology* **164:** 160.

Vollmer NL, **Viricel A**, **Wilcox L**, **Moore MK**, **Rosel PE. 2011.** The occurrence of mtDNA heteroplasmy in multiple cetacean species. *Current Genetics* **57:** 115–131.

Walker JL, **Potter CW**, **Macko SA. 1999.** The diets of modern and historic bottlenose dolphin populations reflected through stable isotopes. *Marine Mammal Science* **15:** 335–350.

Wang J. 2002. An estimator for pairwise relatedness using molecular markers. *Genetics* **160:** 1203–1215.

Wang J. 2007. Triadic IBD coefficients and applications to estimating pairwise relatedness. *Genetics Research* **89:** 135–153.

Waring GT, **Josephson E**, **Fairfield-Walsh CP**, **Maze-Foley K. 2009.** US Atlantic and Gulf of Mexico marine mammal stock assessments—2008. *NOAA Technical Memorandum NMFS-NE* **210**. Available at: https://repository.library.noaa.gov/view/noaa/3630.

Weir BS, **Cockerham CC. 1984.** Estimating *F*-statistics for analysis of population structure. *Evolution; international journal of organic evolution* **38:** 1358–1370.

Wells R, **Scott MD. 1999.** Bottlenose dolphin – *Tursiops truncatus* (Montagu, 1821). In: Ridgway SH, Harrison R, eds. *Handbook of marine mammals*, *Vol. 6.* San Diego: Academic Press, 137–182.

Wickham H. 2016. *Ggplot2: elegant graphics for data analysis*. New York: Springer-Verlag.

Wilkins JS. 2009. *Species: a history of the idea*. Berkeley: University of California Press.

Wilson GA, **Rannala B. 2003.** Bayesian inference of recent migration rates using multilocus genotypes. *Genetics* **163:** 1177–1191.

Yeates DK, **Seago A**, **Nelson L**, **Cameron SL**, **Joseph L**, **Trueman JWH. 2011.** Integrative taxonomy, or iterative taxonomy? *Systematic Entomology* **36:** 209–217.

Zhou X, **Guang X**, **Sun D**, **Xu S**, **Li M**, **Seim I**, **Jie W**, **Yang L**, **Zhu Q**, **Xu J**, **Gao Q. 2018.** Population genomics of finless porpoises reveal an incipient cetacean species adapted to freshwater. *Nature Communications* **9:** 1276.

SUPPORTING INFORMATION

Additional Supporting Information may be found in the online version of this article at the publisher's web-site:

Table S1. List of information for the stranding and biopsy samples of *Tursiops truncatus* of the western North Atlantic used in this study.
Table S2. List of cranial and vertebral measurements, tooth counts and categorical variables analysed in this study. CRCA: *Crassicauda* sp.
Table S3. List of cranial landmarks used in the geometric morphometric analysis.
Table S4. List of the 19 microsatellite loci used in this study, their respective multiplexes and primer concentrations.
Table S5. Information about the mitochondrial DNA control region haplotype sequences of the western North Atlantic (wNA) obtained from GenBank.
Table S6. List with information about the samples of *Tursiops truncatus* collected outside the western North Atlantic and used in this study for the worldwide morphological analyses.
Table S7. List of sequences of *Tursiops* used in the maximum likelihood tree.
Table S8. Total number of individuals assigned to the offshore or coastal bottlenose dolphin ecotypes of the western North Atlantic when considering the five morphological characters.
Table S9. Confusion matrix from random forest models classifying skulls of known live locality and physically mature vertebral columns to a bottlenose dolphin ecotype in the western North Atlantic.
Table S10. Loadings on first two principal components (PC1 and PC2) of the principal components analysis (PCA) using 25 cranial variables.
Table S11. Mean decrease in accuracy importance scores and permutation *P*-values from random forest model for the skull.
Table S12. Summary of the 19 cranial measurements per bottlenose dolphin ecotype of the western North Atlantic.
Table S13. Mean decrease in accuracy importance scores and permutation *P*-values from random forest model for the vertebral column.
Table S14. Confusion matrix from random forest models: sexual dimorphism.
Table S15. Mean decrease in accuracy importance scores and permutation *P*-values from random forest models for sexual dimorphism on skull.
Table S16. Summary of the 19 cranial measurements per bottlenose dolphin ecotype (coastal and offshore) and sex (female and male).
Table S17. Median values of tooth counts for each tooth row in the maxilla (TUL, TUR) and mandible (TLL, TLR) per ecotype.
Table S18. Two-way ANOVA testing for differences in total body length (TL) between physically mature bottlenose dolphins of the western North Atlantic.
Table S19. Assignment probabilities of type specimens to coastal and offshore bottlenose dolphins of the western North Atlantic.
Table S20. Procrustes ANOVA testing for common and unique allometries (three-dimensional geometric morphometrics) between bottlenose dolphin ecotypes of the western North Atlantic.
Table S21. Three-way Procrustes ANOVA testing the effect of skull size (lnCS), ecotypes (coastal and offshore), sex (females and males) and their interactions on skull shape (Procrustes coordinates) of bottlenose dolphins of the western North Atlantic.
Table S22. Confusion matrix from random forest model classifying to an ecotype based on skull shape the skulls of bottlenose dolphin ecotypes in the western North Atlantic.
Figure S1. Diagnostic cranial characters between the coastal and offshore bottlenose dolphin ecotypes of the western North Atlantic.
Figure S2. Decision graphs of the density clustering analyses.
Figure S3. Density clustering δ/ρ, γ and multidimensional scaling plots for skull of all samples.
Figure S4. Density clustering δ/ρ, γ and multidimensional scaling plots for vertebral column samples.
Figure S5. Violin plots of the cranial measurements that best explain the differentiation between ecotypes (see Supporting Information, Table S11) for each ecotype per sex.
Figure S6. Receiver operating characteristic (ROC) curve evaluating the diagnostic ability of classifying the ecotypes based on tooth counts (per tooth row).
Figure S7. Scatter plot of the principal component 1 (PC1) and 3 (PC3) scores based on 23 cranial landmarks and 90 samples.
Figure S8. Mean deviance information criterion (DIC) values of the TESS analyses and Evanno (ΔK) and mean loglikelihood of the data [LnP(D)] plots of the STRUCTURE analyses.

Figure S9. Membership probabilities of bottlenose dolphins in the western North Atlantic based on 19 nuclear microsatellite loci and inferred for $K = 3$ using STRUCTURE (A) and TESS (B).
Figure S10. Density clustering δ/ρ, γ and multidimensional scaling plots for the skull analysis of the global bottlenose dolphin data set.
Figure S11. Phylogenetic tree of bottlenose dolphins based on maximum likelihood methodology.